HHS Public Access

Author manuscript

Glia. Author manuscript; available in PMC 2023 March 01.

Published in final edited form as:

Glia. 2022 March ; 70(3): 430–450. doi:10.1002/glia.24100.

Blocking Kallikrein 6 Promotes Developmental Myelination

Hyesook Yoon[1], **Erin M. Triplet**[2], **Whitney L. Simon**[1], **Chan-Il Choi**[1], **Laurel S. Kleppe**[1], **Elena De Vita**[3,4], **Aubry K. Miller**[4,5], **Isobel A. Scarisbrick**[*,1,2,6]

[1]Department of Physical Medicine and Rehabilitation, Mayo Clinic School of Biomedical Sciences Rochester 55905

[2]Regenerative Sciences Program, Mayo Clinic School of Biomedical Sciences Rochester 55905

[3]University of Heidelberg, Faculty of Biosciences, 69120 Heidelberg, Germany

[4]German Cancer Research Center (DKFZ), 69120 Heidelberg, Germany

[5]German Cancer Consortium (DKTK), 69120 Heidelberg, Germany

[6]Department of Physiology and Biomedical Engineering, Minnesota USA 55905

Abstract

Kallikrein related peptidase 6 (Klk6) is a secreted serine protease highly expressed in oligodendrocytes and implicated in demyelinating conditions. To gain insights into the significance of Klk6 to oligodendrocyte biology, we investigated the impact of global Klk6 gene knockout on CNS developmental myelination using the spinal cord of male and female mice as a model. Results demonstrate that constitutive loss of Klk6 expression accelerates oligodendrocyte differentiation developmentally, including increases in the expression of myelin proteins such as MBP, PLP and CNPase, in the number of CC-1+ mature oligodendrocytes, and myelin thickness by the end of the first postnatal week. Co-ordinate elevations in the pro-myelinating signaling pathways ERK and AKT, expression of fatty acid 2-hydroxylase, and myelin regulatory transcription factor were also observed in the spinal cord of 7d Klk6 knockouts. LC/MS/MS quantification of spinal cord lipids showed sphingosine and sphingomyelins to be elevated in Klk6 knockouts at the peak of myelination. Oligodendrocyte progenitor cells (OPCs)-derived from Klk6 knockouts, or wild type OPCs-treated with a Klk6 inhibitor (DFKZ-251), also showed increased MBP and PLP. Moreover, inhibition of Klk6 in OPC cultures enhanced brain derived neurotrophic factor-driven differentiation. Altogether, these findings suggest that oligodendrocyte-derived Klk6 may operate as an autocrine or paracrine rheostat, or brake, on pro-myelinating signaling serving to regulate myelin homeostasis developmentally and in the adult. These findings document for the first time that inhibition of Klk6 globally, or specifically in oligodendrocyte progenitors, is a strategy to increase early stages of oligodendrocyte differentiation and myelin production in the CNS.

[*]**Correspondence to:** Isobel A. Scarisbrick Ph.D., Neuroscience Program, Physical Medicine & Rehabilitation, Center for MS & Autoimmune Neurology, 642B Guggenheim Building, Mayo Clinic Rochester, 200 First St., SW., Rochester, MN 55905, Tel: 507-284-0124, Scarisbrick.Isobel@mayo.edu.

Competing Financial Interests: The authors declare no competing interests.

Introduction

The process of developmental myelination and the maintenance of myelin integrity in the adult CNS allows for rapid and energy-efficient conduction of action potentials and hence is tightly controlled. Myelinating oligodendroglia not only produce myelin, but also provide critical trophic and metabolic axon support (Stassart et al. 2018). Oligodendroglia are vulnerable to injury in a variety of neurological conditions, leading to conduction block, axonopathy and permanent neurologic impairment. Myelin loss is a hallmark of multiple sclerosis (MS) pathogenesis and congenital leukodystrophies may manifest as developmental hypomyelination or demyelination. Increasing evidence suggests that compromised myelin integrity is also a key component of other neurological conditions, including Alzheimer dementia, Huntington, stroke and spinal cord injury. In MS, ongoing axonal protection and long-term recovery of function depend in part on the ability of oligodendrocyte progenitor cells (OPCs) to replace lost myelin sheaths. There is evidence to support an innate potential for myelin repair in the adult CNS and indeed axon remyelination is observed in some, but far from all, MS lesions (Yeung et al. 2019).

Factors regulating successful myelin regeneration, including the identification of barriers, are only beginning to be understood. The deregulation of environmental factors that either positively or negatively regulate OPC differentiation are of particular interest for therapeutic considerations. Changes in microenvironmental growth factor availability, extracellular matrix molecules, cytokines and chemokines, as well as proteases of several classes, are all considered among key regulators myelin production (Bergles and Richardson 2015; Elbaz and Popko 2019).

Kallikrein-related peptidase 6 (Klk6), also referred to as Zyme (Little et al. 1997), Neurosin (Yamashiro et al. 1997), Protease M (Anisowicz et al. 1996) or Myelencephalon specific protease (MSP) (Scarisbrick et al. 1997a) (see (Scarisbrick and Blaber 2012) for review) is the most abundant serine protease in the adult brain and spinal cord (Scarisbrick et al. 2006a; Scarisbrick et al. 2001; Scarisbrick et al. 1997a). There are studies demonstrating up regulation of Klk6 in the context of traumatic (Radulovic et al. 2013; Radulovic et al. 2016; Scarisbrick et al. 2006b; Yoon et al. 2013), excitotoxic (Scarisbrick et al. 1997a), infectious (Panos et al. 2014; Scarisbrick et al. 2012b), hemorrhagic (Uchida et al. 2004) and inflammatory CNS disorders (Blaber et al. 2004; Scarisbrick et al. 2011; Scarisbrick et al. 2008), including in multiple sclerosis lesions (Scarisbrick et al. 2002). Studies to date suggest Klk6 is positioned to not only modify ECM proteins such as laminin, fibronectin and aggrecan (Bernett et al. 2002; Blaber et al. 2002; Scarisbrick et al. 2006b), but also to activate cell signaling by activation of protease activated receptors (PARs) (Oikonomopoulou et al. 2006; Vandell et al. 2008). The ability of Klk6 to activate Ca^{2+}, extracellular signal related kinase 1/2 (ERK1/2), protein kinase B (AKT) and other intracellular signaling intermediates across the neuron (Vandell et al. 2008; Yoon et al. 2013), astrocyte (Radulovic et al. 2016; Scarisbrick et al. 2012a; Yoon et al. 2018), oligodendrocyte (Burda et al. 2013; Yoon et al. 2015; Yoon et al. 2017) and neuroimmune compartments (Scarisbrick et al. 2011) is linked to its ability to cleave thereby activating protease activated receptors 1 or 2 (PAR1 or PAR2). These receptors permit Klk6 to operate as a hormone-like messenger signaling to cells changes in the extracellular proteolytic

environment. Although Klk6 is positioned to play roles in both CNS homoeostasis and pathogenesis, its neural cell-specific effects remain poorly understood.

Several key lines of evidence link Klk6 to oligodendrocyte biology. First, this trypsin-like secreted serine protease is densely expressed by oligodendrocytes in rodent (Scarisbrick et al. 2000; Scarisbrick et al. 1997a; Yamanaka et al. 1999) and human brain (Scarisbrick et al. 2001). In excess, studies to date demonstrate Klk6 promotes oligodendrogliopathy, but without promoting apoptosis (Scarisbrick et al. 2002). Excess Klk6 also directly suppresses the expression of the major myelin proteins PLP and MBP by primary oligodendrocyte progenitors in culture (Burda et al. 2013). In these studies, the ability of Klk6 to impede oligodendrocyte differentiation was dependent, at least in part, on activation of PAR1. Notably, mice with constitutive knockout of either PAR1 or PAR2 show accelerated myelin development. Moreover, PAR1 knockout mice exhibit accelerated myelin regeneration in acute (lysolecithin) or chronic (cuprizone) models of experimental demyelination (Yoon et al. 2020). Conversely, Murakami et al., 2013 reported developmental reductions in myelination in global Klk6 knockout mice. Collectively, these findings suggest Klk6 is positioned to serve as a regulator of oligodendrocyte differentiation, however it's *in vivo* roles, developmentally and in the adult remain unclear.

In the studies described in this paper, we test the hypothesis that Klk6 plays an inhibitory role in developmental CNS myelination. To test this hypothesis, we investigated the timing of myelination onset, the abundance of myelin at the peak of myelination and in adulthood, and any impact on pro-myelinating signaling pathways using developmental myelination of the murine spinal cord as a well-defined myelinating system. We also investigated associated changes in lipid species in the myelin compartment compared to whole spinal cord extracts using quantitative LC-MS/MS assays. Coupled with an investigation of the ability of OPCs purified from Klk6 knockout mice — or those treated with a novel Klk6 small-molecule inhibitor — to differentiate *in vitro*, our findings suggest that Klk6 is positioned to serve as an innate inhibitor of CNS myelin production. Specifically, findings show for the first time that switching off Klk6 *in vivo* enhances myelination in the early postnatal period, including myelin thickness. Moreover, switching off Klk6 in OPC cultures genetically or pharmacologically, enhances production of the major myelin proteins, MBP and PLP at the early stages of differentiation. Together, these studies highlight Klk6 as a negative regulator of oligodendrocyte differentiation at early stages of development and place this secreted serine protease squarely in the domain of myelin regulatory factors to be considered as a target for disorders of myelin development, injury and disease.

Materials and Methods

Animal care and use

Mice genetically deficient in Klk6, or wild type litter mates, were used in all *in vivo* experiments. Both male and female mice were used and ranged in age from postnatal day (P) 0 to 90 days. Coding exons 3 and 4 of the Klk6 gene were deleted in knockouts by inserting a "universal docking site" cassette (Samantha Sykioti et al. 2020) (Dr. A. Nagy, Mount Sinai, Toronto, Canada) and were a generous gift from Dr. G. Sotiropoulou, University of Patras, Greece. A schematic diagram of the transgenic cassette and the PCR

genotyping strategy were recently published (Pampalakis et al. 2017). Mice with Klk6 knockout are viable, fertile and have no prominent phenotypic abnormalities. Wild-type (Klk6+/+) littermates were used as controls for all experiments. Mice were genotyped using probes and primers as listed in Table 1, using iTaq™ Universal Probes One-Step Kit or the iTaq™ Universal SYBR Green One-Step Kit (1725141 or 1725151, respectively, Bio-Rad) on a CFX96 Touch Real-Time PCR Detection system machine (Bio-Rad). Klk6 knockout, Klk6 wild type and C57BL/6J mice (#000664, Jackson Laboratory Bar Harbor, ME) were used for the study of Klk6 in primary oligodendrocyte progenitor cell cultures. All animal experiments were carried out with adherence to NIH Guidelines for animal care and safety and were approved by the Mayo Clinic Institutional Animal Care and Use Committee.

RNAscope and quantitative PCR

To confirm the presence or absence of Klk6 expression, spinal cords from Klk6 knockout or wild type mice were examined for RNA expression by *in situ* hybridization using RNAscope 2.5 HD Duplex reagents (#322430, Advanced Cell Diagnostics, Newark, CA). All assays were carried out per manufacturer's instructions. The C1-tagged Klk6 (Mm-Klk6, 493751-C1) probe was visualized using horseradish peroxidase-based green chromogenic development. Sections were counterstained with hematoxylin and cover slipped with Vectamount (H5000, Vector Labs, Burlingame, CA). Stained tissue sections were captured digitally (Olympus BX51 microscope and DP72 camera equipped with CellSens software 1.9).

Quantitative real time PCR was used to evaluate the impact of Klk6 on the expression of myelin-associated genes (myelin basic protein (*Mbp*), proteolipid protein (*Plp*), 2',3'-Cyclic-nucleotide 3'-phosphodiesterase (*Cnpase*), oligodendrocyte transcription factor 2 (*Olig2*), myelin regulatory factor (*Myrf*), fatty acid 2 hydroxylase (*Fa2h*) and galactosyltransferase 8A (*Ugt8a*)). RNA was isolated from 3 to 4 whole spinal cords from individual Klk6+/+ or Klk6−/− male and female mice on postnatal day (P) 0, 7, 21, 45 and 90 using RNA STAT-60 (Tel-Test, Friendswood, TX). Alternatively, RNA was isolated from freshly purified OPCs (0 h) or after a 72 h period of differentiation in defined media (see cell culture section below). The relative amount of RNA in each case was determined in 0.1 μg of RNA using an iCycler iQ5 system (BioRad) with probes (Thermo Fisher Scientific, Waltham, MA; or Integrated DNA Technologies, Coralville, IA) or primers (Integrated DNA Technologies, Coralville, IA) listed in Table 1.

Oligodendrocyte quantification in the developing mouse spinal cord

To evaluate whether the Klk6-regulated changes in myelin proteins and myelin gene expression reflect changes in the number of OPCs or mature oligodendroglia, we enumerated Olig2 (Ab9610; AB_570666, Millipore) or CC-1 (anti-adenomatous polyposis coli (APC), Ab16794; AB_443473, Abcam, Cambridge, MA) immunopositive cells in 6 μm paraffin sections through the dorsal columns or ventrolateral white matter of male and female P0, 7, 21, 45 and 90 spinal cords. Olig2 is a basic helix-loop-helix transcription factor expressed by OPCs and oligodendroglia at the early stages of differentiation, whereas CC-1 is associated only with the mature phenotype. Counts were made from stained sections that were digitally imaged under constant illumination (Olympus BX51 microscope,

Olympus, Center Valley, PA) using a DP72 camera equipped with CellSens software 1.9 (Olympus, Center Valley, PA).

Quantification of myelin protein expression using Western blot

Western blots were used to quantify myelin-associated proteins and the pro-myelinating signaling intermediates, AKT and ERK1/2. Whole spinal cord was harvested from 3–4 individual Klk6+/+ or Klk6−/− mice male and female mice on postnatal day (P) 0, 7, 21, 45 and 90. Spinal cords at each time point were collectively homogenized in radio-immunoprecipitation assay buffer and 25 μg of protein resolved on sodium dodecyl sulfate-polyacrylamide gels (Bio-Rad Laboratories, Hercules, CA). Multiple electroblotted membranes were used to sequentially probe for antigens of interest, including myelin proteins PLP (Ab28486; AB_776593, Abcam, Cambridge, MA), MBP (MAB386; AB_94975, Chemicon, Billerica, MA), and CNPase (MAB326; AB_2082608, Millipore, Billerica, MA); oligodendrocyte proteins, Olig2 (Ab9610; AB_570666, Millipore); or the phosphorylated or total protein forms of ERK1/2 (9101S; AB_331646, 9102S; AB_330744, Cell signaling, Boston, MA) and AKT (4058L; AB_331168, 9272S; AB_329827, Cell signaling). Membranes were also re-probed for β-actin (NB600–501, Novus Biological, Littleton, CO, USA) to further control for loading. The relative optical density (ROD) of each protein of interest was normalized to that of actin or in the case of pERK1/2 or pAKT to total ERK1/2 or AKT, respectively. The mean and standard error (s.e.) of ROD readings across at least 3 independent Westerns for each antigen of interest was used for statistical comparison fs (Yoon et al. 2013).

Quantification of myelin thickness

The number of myelinated axons and the thickness of myelin sheaths were determined by ultrastructural analysis of the spinal cord dorsal column white matter and ventral lateral white matter of Klk6+/+ (n=3 males/2 females); and Klk6−/− (n=3 males/3 females) at P7. Mice were perfused with Trump's fixative (4% formaldehyde with 1% glutaraldehyde pH 7.4) and a 1 mm segment of the cervical spinal cord was osmicated and embedded in araldite. All myelinated axon counts for each genotype were averaged across 5 to 6 (mixed with male and female) independent animals per genotype. Myelin sheath thickness in the dorsal column and ventral lateral white matter of the cervical spinal cord at P7 was quantified in ultrathin (0.1 mm) sections taken from araldite blocks using a JEM-1400 Transmission Electron Microscope (JEOL USA, Peabody, MA). Images were captured at 8,000X without knowledge of genotype and included five fields across the dorsal and five fields in the ventral lateral white matter. G-ratios were calculated from all myelinated axons in each image and this included axons with diameters ranging from 0.5 to 3 μm. Across 5 – 6 animals per time point this resulted in measurement of roughly 1000 myelinated axons for each genotype per region. Measurements of axon diameter (d) and myelin fiber diameter (D) were made by including axons of all diameters using Image J software and presented as mean g-ratio (d/D) or myelin thickness ± SE across axon diameters. As very few axons were ≥ 3 μm, the mean values calculated in each case were essentially identical to those when only axons < 3 μm were included. This analysis parallels methods used in in prior studies (Furusho et al. 2012; Ishii et al. 2013; Ishii et al. 2012; Yoon et al. 2017), facilitating comparison of results.

Quantification of spinal cord lipids and cholesterol

To quantify any changes in lipids in the spinal cord or purified myelin membranes of Klk6 knockouts compared to wild types, we used a targeted liquid chromatography with tandem mass spectrometry (LC-MS/MS) approach, focusing on identification of CNS-enriched lipids. Gas chromatography mass spectrometry (GCMS) was used to quantify free and bound cholesterol (Paik et al., 2008). A total of 8 female mice from each genotype at either postnatal day 21 or 60 were euthanized, perfused with saline, and spinal cords harvested. Five spinal cords were used for detection of lipid species and cholesterol directly and three were used to first purify myelin membranes by sucrose-gradient ultracentrifugation (Norton and Poduslo 1973) prior to downstream analysis. All assays were performed using previously published protocols at the Mayo Clinic Metabolomics Core Facility, including GCMS quantification of free and bound cholesterol (Paik et al. 2008), LC-MS/MS quantification of glucosyl/galactosyl ceramides, ceramides and sphingomyelins (Blachnio-Zabielska et al. 2012; Boutin et al. 2016).

Myelin protein expression by OPCs and oligodendroglia *in vitro*

Primary oligodendrocyte progenitor (OPCs) cultures of greater than 95% purity were prepared from postnatal day 1 to 3 mixed glial cultures from male and female mice, as previously described (Burda et al., 2013; Yoon et al., 2015). Briefly, mixed glial cultures were grown in Dulbecco's Modified Eagle Medium (DMEM) (11960–044, Gibco), containing 1 mM sodium pyruvate (11360070, Corning), 20 mM 4-(2-hydroxyethyl)-1-piperazineethanesulfonic acid (HEPES) (15630–080, Gibco), 10% heat inactivated fetal bovine serum (Atlanta Biologicals, Lawrenceville, GA), 100 U/ml penicillin and 100 μg/ml streptomycin (15140122, Life Technologies), and 5 μg/ml insulin (12585014, Gibco). OPCs were separated from mixed cultures at 10–12 days *in vitro* (DIV) by overnight shaking and were then purified from any contaminating microglia in the retained supernatant by sequential panning on non-tissue culture treated plastic. To determine the impact of Klk6 gene knockout on OPC differentiation, purified OPCs from wild type or Klk6 knockout mice were plated at a density of $4.7 \times 10^4/cm^2$ on PLL-coated 12 mm glass cover slips. OPCs were grown for an additional 24 or 72 h in defined differentiation media consisting of Neurobasal A media (10888022, Life Technologies) containing 1% N2 (17502048, Life Technologies), 2% B27 (17504044, Life Technologies), 100 U/ml penicillin and 100 μg/ml streptomycin (15140122, Life Technologies,), 1 mM sodium pyruvate (11360070, Corning), 0.45% glucose (G8769, Sigma), 2 mM glutamax (35050–061, Fisher), 5% BSA (A4503–100G, Sigma), 50 μM beta-mercaptoethanol (21–031-CV, Fisher), and 40 ng/ml T3 (T6397, Sigma-Aldrich). In some cases, 5-ethynyl-2-deoxyuridine (EdU, 10 μM) was included in the culture media to determine changes in proliferation. All cell culture conditions were performed in triplicate and repeated at least 2 times using independent cell culture preparations.

After 24 or 72 h in differentiation media, coverslips were fixed with 2% paraformaldehyde (PFA) for downstream immune localization of myelin-associated markers. Oligodendrocyte cultures were stained for MBP (1:750, MAB386, Millipore), PLP (1:750, Ab28486, Abcam) and Olig2 (1:200, MABN50, Millipore) using immunofluorescence, nuclei co-labeled with DAPI (4',6-Diamidino-2-Phenylindole, Dihydrochloride) (D1306, Thermo Fisher Scientific)

and cells cover slipped with Fluoromount-G Mountant (0100–01, SouthernBiotech). Five random fields for each coverslip were captured digitally at 20X with an Olympus BX51 microscope and XM10 camera equipped with CellSens software 1.9, under constant illumination. Image J software was used to determine the total area of PLP or MBP staining and the number of Olig2+ or EdU+ cells.

To validate findings that purified OPCs with genetic Klk6 gene knockout show enhanced differentiation, we next investigated if a Klk6 small molecule inhibitor would replicate these effects. To accomplish this, purified OPCs derived from C57BL/6J mice were plated 4.7 $\times 10^4/cm^2$ on PLL coated glass cover slips in defined differentiation media, as described above. These Klk6+/+ OPC cultures were treated with a Klk6 small molecule inhibitor, DKFZ-00251 (100 or 500nM, provided by Dr. A. Miller, German Cancer Research Center (DKFZ), Heidelberg) (De Vita et al. 2018) or vehicle (DMSO) alone. To investigate the potential impact of Klk6 inhibition on OPC proliferation, EdU was included in the media and coverslips were fixed with 3.7% formaldehyde and processed using Click-iT (Alexa Fluor 555) to detect EdU labeled cells according to the manufacturer's instructions (Life Technologies) prior to immune localization of MBP, PLP, and Olig2 (Yoon et al. 2020). To investigate any beneficial effects of blocking Klk6 function on the ability of BDNF to promote oligodendrocyte differentiation, as we recently observed for PAR1 inhibition (Yoon et al., 2020), brain-derived neurotropic factor (BDNF, 1ng/ml, 450–02-2, Peprotech) was included in the culture media in some cases. Following a 24 or 72 h period of differentiation, coverslips were fixed and cells stained for myelin markers and EdU as described above.

Statistical comparisons

All data are expressed as mean ± s.e.m. Comparisons between multiple groups were made using a One-Way Analysis of Variance (ANOVA) and the Newman Keuls post-hoc test. When data for multiple comparisons were found not to be normally distributed, the Kruskal-Wallis ANOVA on Ranks was applied with Dunn's method. For pairwise comparisons between two groups, the Students unpaired t-test was used. For targeted lipidomics data, comparisons between P21 and P90 for spinal cord and myelin were assessed for statistically significant differences using Student's t-test to obtain a p-value for each sample, and then p-values were adjusted using the Benjamini-Hochberg Procedure with a false-discovery rate of 0.05 to correct for multiple comparisons. Statistical significance was set at $P < 0.05$.

Results

Klk6 gene knockout accelerates developmental myelin-associated gene expression.

Klk6 gene expression—To investigate the role of Klk6 in CNS myelination, we compared the expression of *Klk6* and key signatures of myelination in the spinal cord of wild type and Klk6 knockout mice from birth (postnatal day 0, P0) to maturity (P90) (Figure 1). Myelination of the rodent spinal cord occurs largely postnatally with peak numbers of myelinating cells and expression of the major myelin proteins (MBP and PLP), occurring by P21. First, we quantified the developmental expression of *Klk6* RNA in the spinal cord and demonstrate this to be lowest at birth (6.4E+05 ± 8.4E+04 copies/100 ng of RNA), with progressive increases that reach 6.4E+07 ± 3.8E+06 copies/100 ng of RNA at the P21

peak of myelination. This represents a 56-fold increase in *Klk6* expression in the spinal cord between P0 to P7 and an 801-fold increase between P0 and P21. *Klk6* expression was not detectable by PCR in RNA purified from the spinal cords of Klk6 knockout mice. We also used *in situ* hybridization to demonstrate dense expression of *Klk6* in spinal cord white matter of wild type mice and a complete absence of expression in Klk6 knockout mice.

Myelin gene expression—Using quantitative PCR approaches, we document that the spinal cord of Klk6 knockout mice expresses 30 to 40% higher levels of each of the major myelin proteins (*Mbp* and *Plp*) by P7 compared to wild types ($P < 0.001$ and $P = 0.02$, respectively, Neuman Keuls (NK)) (Figure 1). In addition, expression of the oligodendrocyte transcription factor 2 (*Olig2*) that is expressed by oligodendrocyte progenitors and young oligodendrocytes was also increased by P7 in the spinal cord of Klk6 knockouts compared to wild types ($P < 0.001$, NK). Coupled with these findings, Klk6 knockouts showed an accelerated pattern of myelin regulatory factor (*Myrf*) expression by P7 ($P < 0.001$, NK). Myrf is a transcription factor absolutely critical for developmental myelination (Bujalka et al. 2013). Reflecting accelerated expression of each of these key indices of myelination in Klk6 knockout spinal cords by P7, thereafter, knockouts more quickly reached levels of expression achieved and maintained in the mature state.

Lipid gene expression—Given the lipid-rich nature of the myelin membrane (approximately 70% lipid by weight), we next examined two enzymes involved at key intersections in the production pathways of lipids of significance to myelin (Figure 1). Fatty acid 2-Hydroxylase (*Fa2h*), an enzyme that catalyzes the hydroxylation of free fatty acids to generate 2-hydroxyl fatty acids, the building blocks of sphingolipids and glycosphingolipids, was elevated by 1.9-fold in Klk6 knockouts on P7 ($P \leq 0.001$, NK). Mutations in Fa2h are associated with leukodystrophy, dysmyelination with spastic paraparesis and neurodegeneration (Dick et al. 2010). UDP glycosyltransferase 8 (*Ugt8a*), which catalyzes the transfer of galactose to ceramide, a key enzymatic step in the biosynthesis of galactocerebrosides abundant in myelin membranes, trended to higher levels at P7 in Klk6 knockouts, but did not reach statistical significance.

Klk6 gene knockout accelerates early oligodendrocyte differentiation.

To address the actions of Klk6 in regulating the number of oligodendrocytes and their differentiation, we enumerated Olig2+ progenitors and anti-adenomatous polyposis coli clone positive (CC-1+) mature oligodendrocytes across the dorsal and ventrolateral regions of spinal cord white matter from P0 to P90 (Figure 2). By P7, Klk6 knockouts already showed greater numbers of CC-1+ mature oligodendrocytes (2.7-fold in the dorsal column ($P < 0.001$, NK) and 1.6-fold in the ventrolateral white matter ($P = 0.001$, NK)) relative to wild type comparators. The increases in counts of mature CC-1+ oligodendrocytes in Klk6 knockouts persisted to the P21 peak of myelination. At P21, Olig2 levels were correspondingly decreased ($P = 0.02$, NK). The number of Olig2 and CC-1+ oligodendrocytes did not differ across genotypes by P90.

Klk6 gene knockout accelerates myelin-associated protein expression and pro-myelinating signaling.

Myelin protein expression—To determine if the early (P7) developmental increases in *Mbp* and *Plp* RNA and CC-1+ oligodendrocytes observed in the spinal cord of Klk6 knockout mice are reflected in parallel increases in expression of the major myelin proteins, MBP and PLP, we quantified each of these, in addition to Olig2 and CNPase in protein homogenates prepared from the P0 through P90 spinal cord (Figure 3). MBP protein was elevated by 1.2-fold in the spinal cord of Klk6 knockout mice compared to wild types at P7 ($P = 0.04$, NK). Both PLP and CNPase protein expression trended to elevated levels at P7; however, these 1.2- to 1.6-fold changes, respectively, did not reach the level of significance ($P = 0.9$ and $P = 0.6$, respectively, NK). Overall, Olig2 protein levels were not elevated in Klk6 knockout spinal cords early and showed lower levels compared to wild types by P21 through P90 ($P = 0.01$ at P21, $P < 0.001$ at P45 and $P = 0.002$ at P90, NK).

AKT and ERK1/2 signaling—Increases in signaling through the AKT and ERK1/2 pathways is known to enhance myelin production (Czopka et al. 2010; Fyffe-Maricich et al. 2013; Guardiola-Diaz et al. 2012; Harrington et al. 2010; Ishii et al. 2013; Ishii et al. 2012). It is therefore noteworthy that levels of activated AKT and ERK1/2 were each elevated at P7 in Klk6 knockouts (Figure 4). These increases in pro-myelinating signaling pathways occur in parallel to the increases in oligodendrocyte differentiation (CC-1) and MBP RNA and protein expression, also observed in independent P7 spinal cord samples (Figures 1 and 2). By P45 and at P90, no differences in AKT signaling were seen across genotypes, but total ERK1/2 was elevated at P45 and activated ERK1/2 reduced in Klk6 knockouts by P90 ($P = 0.01$ and $P = 0.04$, respectively, NK).

Klk6 gene knockout results in early increases in myelin thickness.

Given the acceleration of signs of myelination by the end of the first postnatal week, we used ultrastructural approaches to quantify the number of myelinated axons and myelin thickness at P7 (Figure 5). Approximately 70% of all axons in the dorsal column and ventrolateral white matter ranged from 1 to 3 μm in diameter and this is where we saw the most significant increases in myelin thickness in Klk6−/− compared to wild type mice. Mean g-ratios in dorsal column were smaller in Klk6−/− (0.92 ± 0.0009) compared with Klk6+/+ (0.93 ± 0.0009, $P = 3.3 \times 10^{-11}$, Student's t-test). A decrease in dorsal column white matter g-ratios in the Klk6−/− spinal cord was reflected in significantly thicker myelin sheaths across all axon diameters (Klk6−/− = 0.11 ± 0.001 μm; Klk6+/+ = 0.089 ± 0.001 μm, $P = 2.6 \times 10^{-18}$, Student's t-test). In ventrolateral white matter, the mean g-ratio and myelin thickness of axons were not significantly different in Klk6−/− compared with Klk6+/+ mice. Although there was a trend toward an increase in the number of myelinated axons in dorsal column and ventral lateral white matter of Klk6−/−, this did not reach the level of statistical significance.

Klk6 knockout increases CNS lipid production at the peak of myelination.

We used quantitative LC-MS/MS approaches to investigate any impact of Klk6 gene knockout on lipids extracted from the whole spinal cord or from purified myelin membranes

at the P21 peak of myelin production and at P90 (Figure 6, Tables 2 and 3). First, in whole spinal cord, levels of free cholesterol were increased in Klk6 knockouts by 1.4-fold at P21 (P = 0.03, Student's t-test) (Table 2). In lipids extracted from the spinal cord of Klk6 knockouts, the ceramide, sphingosine (Sph) was also elevated by 1.3-fold at P21 (P = 0.02, Student's t-test). In addition, short (SM_C16) and long chain (SM_C24:1) sphingomyelins were elevated by ~1.6 fold (P = 0.01, Student's t-test) in the spinal cord of Klk6 knockout mice at P21. There were no differences by genotype in individual lipid species in whole spinal cord by P90. Some of these same lipid species also trended to be elevated in myelin purified from the spinal cord of Klk6 knockouts at P21 or P90 (e.g. sphingosines and ceramides), but after controlling for multiple comparisons (Benjamini-Hochberg correction) these differences were not significant (Table 3).

Oligodendrocyte progenitors with Klk6 gene knockout show signs of accelerated myelin production *in vitro*.

Given several lines of evidence that Klk6 knockout mice show signs of accelerated myelination (Figures 1 to 4, Tables 2 and 3), we next used purified cultures of OPCs from the cortices of wild type or Klk6 knockout mice to determine the potential direct impact of OPC Klk6 on oligodendrocyte differentiation (Figure 7). First, immunofluorescence techniques revealed 1.5-fold increases in PLP protein per Olig2+ cell in Klk6 knockout OPCs differentiated for 72 h in culture (P = 0.03, Student's t-test). The number of Olig2 positive cells was also increased in OPC cultures lacking Klk6 after 72 h (P = 0.05, Student's t-test). Next, we used quantitative PCR to show that *Klk6* is expressed by wild type OPCs and increases by 1.3-fold (P = 0.03) after 72 h, while also increasing expression of *Mbp* by 3.1-fold (P = 0.00004) and *Plp* by 4.8-fold (P = 0.00005, Student's t-test). We also observed that OPCs purified from Klk6 knockouts already express 1.9-fold higher levels of *Mbp* RNA at the time of isolation (0 h) compared to wild types (P = 0.003). After a 72 h period of differentiation, Klk6 knockout oligodendrocytes express 1.2-fold higher *Mbp* and 5.7-fold higher *Plp* RNA compared to wild types (P = 0.004 and P = 0.00004, respectively, Student's t-test). Conversely, expression of *Olig2* RNA was lower in Klk6 knockout OPCs at both 0 and 72 h in culture (P = 0.02 and P = 0.0008, respectively, Student's t-test). Together, these findings suggest that blocking OPC Klk6 can directly enhance the early stages of OPC differentiation.

Pharmacologic Klk6 inhibition promotes myelin production *in vitro*.

While the increases in myelin production in freshly isolated and differentiated OPCs from Klk6 gene knockout mice is suggestive of a direct – autonomous – effect, these results do not rule out potential effects from other cell types *in vivo* prior to OPC isolation, or *in vitro* during the expansion and panning procedures (Figure 8). Therefore, we used a Klk6 small molecule inhibitor, DFKZ-251 (De Vita et al. 2018; De Vita et al. 2020), applied at the time of plating of wild type OPCs and quantified the number of Olig2+ cells and expression of MBP and PLP proteins at 24 and 72 h time points. First, we observed that wild type OPCs treated for only a 24 h period with the Klk6 inhibitor already showed greater total MBP+ area/Olig2+ cell (1.2-fold, P = 0.02, NK). Counts of Olig2+ oligodendrocytes were also increased (1.5-fold, P = 0.03, NK). 72 h after application of the Klk6 inhibitor to differentiating OPC cultures, inhibitor-driven enhancements in total MBP+ area/Olig2+

oligodendrocyte continued. We observed a 72 h period of DFKZ-251 treatment to drive increases in MBP production in a dose-dependent manner with 1.6-fold increases at 100 nM ($P = 0.003$, NK) and 2.3-fold increases at 500 nM ($P < 0.001$, NK). There was also a non-dose dependent increase in the total number of DAPI-labeled cells in cultures after 72 hr of Klk6 inhibition ($P = 0.01$ at 100 nM and $P = 0.03$ at 500 nM, NK), but not in Olig2 counts. There was a trend for cultures treated with the Klk6 inhibitor for 72 h to increase EdU incorporation, but this did not reach the level of statistical significance.

Pharmacologic Klk6 inhibition enhances the myelin promoting effects of BDNF *in vitro*.

An important mode of Klk6 action is to cleave, thereby activating, either PAR1 or PAR2 to elicit intracellular signaling (Vandell et al. 2008; Yoon et al. 2018). Our recent studies show that genetic blockade of PAR1 or PAR2 increases developmental myelin production in the spinal cord (Yoon et al. 2015; Yoon et al. 2017). Also, either genetic or pharmacologic blockade of these receptors in purified OPC cultures enhances myelin expression and augments the pro-myelin generating effects of BDNF (Yoon et al. 2020; Yoon et al. 2017). Since Klk6 represents a potential innate activator of PAR1 or PAR2, we next investigated possible interactions between Klk6 and BDNF. Specifically, we examined the effects of the Klk6 inhibitor DKFZ-251 on the expression of myelin proteins when applied alone or in combination with suboptimal levels of recombinant BDNF 1 ng/ml (Figure 9). Our findings show that inhibition of Klk6 promotes increases in total MBP+ and PLP+ area / Olig2+ oligodendrocytes to a level similar to that of 1 ng/ml BDNF (~2.2-fold and ~1.7-fold, respectively). Both DKFZ-251 and 1 ng/ml BDNF also increased counts of Olig2 cells over the same 72 h period (1.8-fold and 1.6-fold, respectively). Moreover, the combination of Klk6 inhibition along with supplementation of cultures with 1 ng/ml BDNF drove higher levels of both total PLP+ area per Olig2+ cells (2.3-fold) and Olig2 counts (2.4-fold) compared to either factor alone ($P = 0.001$ and $P = 0.009$, respectively, NK).

Discussion

The identification of factors regulating myelination is critical to the development of a tool kit to treat hypomyelinating and demyelinating conditions of the CNS. Klk6 is a secreted serine protease highly expressed by oligodendroglia, but there is limited information regarding its functional roles. Through an investigation of developmental spinal cord myelination in mice with Klk6 gene knockout, we demonstrate that blocking Klk6 globally accelerates oligodendrocyte differentiation, including production of the major myelin proteins PLP and MBP, production of sphingomyelins, and signaling through the AKT and ERK1/2 pathways during the early postnatal window of rapid spinal cord myelin formation. Coupled with findings that genetic or pharmacologic blockade of Klk6 in purified OPC cultures similarly enhances early stages of oligodendrocyte differentiation and potentiates the pro-myelinating effects of BDNF, these studies identify Klk6 as part of the network of factors orchestrating myelin development and suggest blocking Klk6 as a strategy to enhance pro-myelinating signaling and developmental oligodendrocyte differentiation.

Link between Klk6 expression and developmental myelination.

Oligodendrocyte development is tightly controlled by a myriad of molecular cues, including extrinsic extracellular signals and oligodendrocyte-intrinsic factors, such as transcription factors, epigenetic modulators, miRNAs and signaling pathways (Bergles and Richardson 2015; Elbaz and Popko 2019; Emery and Lu 2015; Wang and Lu 2020). Prior studies show Klk6, a secreted serine protease, is preferentially expressed in the CNS and is enriched in mature oligodendrocytes (Scarisbrick et al. 2000; Scarisbrick et al. 1997b). Data presented point to roles for Klk6 in the process of developmental myelination, with *Klk6* RNA expressed at low levels in the spinal cord at birth, followed by 56-fold increases in the first week, thereafter reaching ~2 log-fold higher levels by the P21 peak of myelination. Both myelin production and *Klk6* levels remain steady thereafter, at least through the P90 end point examined. The association between increasing levels of *Klk6* expression and oligodendrocyte differentiation *in vivo* was mirrored in primary OPC cultures. Furthermore, independent gene profiling of differentiating oligodendrocytes *in vitro* suggests Klk6 is among the most enriched genes in myelin oligodendrocyte glycoprotein+ (MOG+) compared to MOG- oligodendrocytes (Cahoy et al. 2008).

Despite accumulating evidence that Klk6 is enriched in mature oligodendrocytes, the functional relationship between increasing levels of Klk6 and oligodendrocyte maturation is unclear. Prior studies do suggest that Klk6 serves as a negative regulator of oligodendrocyte differentiation. For example, recombinant Klk6 limits the extension of myelin membranes and suppresses the expression of *Mbp* and *Plp* RNA in purified oligodendrocyte cultures (Burda et al. 2013; Scarisbrick et al. 2002). Conversely, other studies report Klk6 siRNA reduces oligodendrocyte MBP production (Bando et al. 2006), with Klk6 knockout mice showing early delays in the abundance of spinal cord MBP (Murakami et al. 2013). To address these opposing views regarding the actions of Klk6 in developmental myelination, we investigated the impact of Klk6 gene knockout on developmental spinal cord myelination using multiple indicators and sought to uncover a possible cellular mechanism. We pair *in vivo* findings with *in vitro* studies demonstrating the impact of genetic or pharmacologic blockade of Klk6 function using highly purified primary OPC cultures.

Supporting a model in which increasing levels of Klk6 expression developmentally suppresses myelin production at P7, markers of mature myelin (*Mbp*, *Plp* and *Cnpase* RNA expression) were all elevated by 1.3–1.4-fold in Klk6 knockouts. Also, at P7, Klk6 knockouts showed higher levels of expression of *Olig2* and *Myrf*, transcription factors that play essential roles in myelination (Bujalka et al. 2013; Ligon et al. 2006). Nearly 2-fold higher levels of *Fa2h* expression, a key enzymatic step in sphingolipid and glycosphingolipid synthesis, were also observed in Klk6 knockouts at P7. Complementing these findings, increased levels of MBP protein were also observed at P7 in the spinal cord of Klk6 knockout mice. Findings that Klk6 gene knockout is associated with an accelerated pattern of early spinal cord myelination are further supported by findings of greater numbers of CC-1+ oligodendrocytes at both P7 and the P21 peak of spinal cord myelination. Interestingly, while clear differences in the number of myelinated axons between genotypes was not seen at P7, the thickness of myelin membranes in Klk6 knockouts was greater than wild type comparators. Coupled with this, LC-MS/MS quantification of lipids in the P21

spinal cord showed free cholesterol— that is the form found active in cell membranes— as well as sphingosine and sphingomyelins were all elevated in Klk6 knockouts. Notably, the function of myelin is tightly linked to its high lipid-to-protein ratio and cholesterol enrichment (Chrast et al. 2011). Each of these lines of evidence suggests Klk6 gene knockout accelerates the early program of developmental myelination. Future studies are needed to address the regulatory links between Klk6 and transcriptional regulators of proteins and lipids essential for myelination of the CNS and the biological significance of these changes.

Our findings suggest that the relative increases in CC-1+ mature oligodendrocytes in the spinal cord of Klk6 knockout mice at P7 and P21 occur in conjunction with a relative decrease in Olig2 counts. Since Olig2 is a marker of OPCs and young oligodendrocytes, reductions with Klk6 knockout lends further support to the body of evidence suggesting that increasing levels of Klk6 developmentally serve as a negative regulator oligodendrocyte differentiation. Given that Klk6 is an activator of PAR1 and PAR2, the increases in mature CC-1+ oligodendrocytes observed in the spinal cord of PAR1 (Yoon et al. 2015) and PAR2 (Yoon et al. 2017) knockouts at a parallel time point (P7) harmonize well, although we cannot rule out other pivotal Klk6 activities. Together, these findings suggest that the absence of Klk6 results in an accelerated program of early spinal cord myelination, possibly through a mechanism that involves reduced signaling at PAR1 and PAR2.

Kallikrein 6 as a negative regulator of pro-myelination signaling pathways.

Through its ability to activate the G-protein coupled receptors PAR1 and PAR2, secreted Klk6 can operate in a hormone-like manner to directly impact the network of signaling pathways regulating myelination. Two signaling pathways with strong links to developmental myelination are AKT and ERK1/2, such that over expression of either promotes hypermyelination, including increases in myelin thickness (Fyffe-Maricich et al. 2013; Ishii et al. 2013; Narayanan et al. 2009). Lending further support to a model in which blocking Klk6 increases the capacity for developmental myelination, we observed elevated signaling in both the AKT and ERK pathways in the spinal cords of Klk6 knockouts at P7, in tandem with increases in myelin-associated RNA and protein expression, and in mature oligodendrocyte numbers. The possibility that Klk6 is a negative regulator of these pathways in part by activating PAR1 and PAR2, is supported by prior findings: PAR1 knockout mice show increased ERK1/2 activation on P0 and P21 and increased AKT on P7 and P21. Knockout of PAR2 promoted increases in ERK1/2 signaling at P7 and P21. Together, these findings support a working model in which knocking out PAR1 or PAR2, or a major agonist of these receptors highly expressed in CNS—Klk6— fosters the program of early developmental myelination.

Autocrine/paracrine action of oligodendrocyte Klk6 as a negative regulator of myelin protein expression.

While the *in vivo* studies we present demonstrating that mice with constitutive knockout of Klk6 function show accelerated developmental spinal cord myelination, these findings do not address the cellular mechanism(s) involved. In addition to expression by OPCs and oligodendrocytes (Scarisbrick et al. 2000; Scarisbrick et al. 1997a), Klk6 is expressed by

neurons and can be up regulated in astrocytes and microglia, particularly in the context of injury and disease (Blaber et al. 2004; Radulovic et al. 2013; Radulovic et al. 2016; Scarisbrick et al. 2002; Scarisbrick et al. 2006b). Therefore, whether Klk6 loss-of-function in OPCs alone would be sufficient to increase pro-myelinating signaling and accelerate developmental myelination will be the subject of future studies when conditional-ready Klk6 mice become available. To begin to address the hypothesis that Klk6 generated by OPCs negatively regulates oligodendrocyte differentiation in an autocrine or paracrine manner, we investigated the ability of wild type or Klk6 knockout OPCs to express *Mbp* and *Plp* upon differentiation in culture. Supporting a model in which Klk6 produced by OPCs operates in an autocrine or paracrine manner to negatively regulate differentiation, Klk6 knockout OPCs already expressed higher levels of *Mbp* RNA at the time of plating, with increases in both *Mbp* and *Plp* by 3 days *in vitro*.

Since findings of increased expression of myelin proteins in Klk6 knockout OPCs does not rule out potential developmental influences *in vivo* prior to culture– or *in vitro* during the mixed glial culture stages used to expand and purify OPCs, we next investigated the impact of a novel Klk6 small molecule inhibitor applied to wild type OPCs at the time of plating. Pharmacologic inhibition of Klk6 in purified OPC cultures increased both MBP and PLP protein area per total Olig2+ cells. Increases in the number of Olig2+ cells and total DAPI counts were also observed in OPC cultures in which the Klk6 inhibitor was included, however increases in EdU incorporation were not significant. Defining any effects of Klk6 inhibition on OPC proliferation, survival or both will require additional study as will an understanding of roles in more mature cultures and myelinating cultures. Altogether with the findings that OPCs with genetic Klk6 loss-of-function also express more myelin proteins, these data suggest increasing levels of Klk6 production by OPCs during maturation may serve in an autocrine or paracrine manner to slow or impede further myelin protein expression. Consistent with this model spinal cord Klk6 is relatively low at early stages of development, with significant increases occurring by the peak of myelination when increases in myelin proteins plateau. Therefore, Klk6 may operate as a rheostat, or brake, on developmental myelin production and support myelin homeostasis in adulthood.

Interplay between Klk6 and BDNF in regulating myelin protein expression.

That knocking out Klk6 unleashes early oligodendrocyte differentiation, suggests a mechanism of negative regulation of pro-myelination signals may be at play. While there are numerous extrinsic signals that promote OPC differentiation, we focus efforts here on BDNF. This focus is driven not only by the robust pro-myelinating effects of BDNF reported to date (Fletcher et al. 2018; Fulmer et al. 2014; Ramos-Cejudo et al. 2015; VonDran et al. 2011; Wong et al. 2013), but also by prior studies showing that the level of activation of PAR1 or PAR2 is inversely related to the ability of BDNF to promote oligodendrocyte differentiation *in vitro* (Yoon et al. 2020; Yoon et al. 2015; Yoon et al. 2017). To test the hypothesis that blocking an innately expressed activator of PARs (Klk6) is permissive for BDNF-mediated OPC differentiation, we investigated whether pharmacologic blockade of Klk6 improves the pro-myelinating potential of suboptimal levels of BDNF. First we found that blockade of Klk6 produced similar increases in total PLP and MBP across Olig2+ cells, and in Olig2 counts, as was observed with suboptimal BDNF (1 ng/ml). Moreover, blockade

of Klk6 in combination with 1 ng/ml BDNF increased PLP+ area per Olig2+ cells and Olig2 counts to a greater extent than either factor alone. While the intracellular signaling cascades impacted that would inform if these are independent or parallel events remains to be determined, taken together with prior studies, these findings suggest that blockade of Klk6, or the receptors Klk6 activates (PAR1 or PAR2) (Yoon et al. 2015; Yoon et al. 2017), is sufficient to improve the efficacy of BDNF-mediated oligodendrocyte differentiation. These findings highlight a new myelin regulatory network involving Klk6-PAR1/2-and BDNF that is positioned to play roles in myelin production at early developmental stages. These findings also suggest that targeting the Klk6-PAR axis may improve the pro-myelinating capacity of growth factors which may be in limited supply in demyelinating conditions affecting the developing and adult CNS.

Prior studies have linked Klk6 to demyelinating conditions, including direct oligodendrogliopathy (Scarisbrick et al. 2002), as well as MBP, MOG and blood brain barrier protein breakdown (Angelo et al. 2006; Bernett et al. 2002; Blaber et al. 2004; Blaber et al. 2002). Roles for Klk6 in CNS pro-inflammatory responses, including increases in immune cell survival (Scarisbrick et al. 2011) and cytokine production (Blaber et al. 2004; Scarisbrick et al. 2011; Scarisbrick et al. 2006b) have also been described. For example, Klk6 is elevated in MS lesions and in serum (Scarisbrick et al. 2008) and CSF (Hebb et al. 2011; Schutzer et al. 2013; Singh et al. 2015) of individuals with MS. Blocking Klk6 ameliorates EAE- (Blaber et al. 2004) and TMEV- (Scarisbrick et al. 2012b) induced demyelinating disease, while administration of recombinant Klk6 exacerbates disease (Yoon and Scarisbrick 2016). Recent studies complement these findings showing mice with global Klk6 gene knockout show reduced clinical scores and spinal cord inflammation in EAE (Bando et al. 2018). Taken with studies showing that Klk6 can directly suppress myelin gene expression (Burda et al. 2013), the current findings suggest that elevated Klk6 in hypomyelinating or demyelinating conditions may serve to directly inhibit myelin production. Whether blocking Klk6 not only prevents demyelination, but also promotes myelin regeneration will be an important line of future investigation.

In conclusion, these studies place Klk6 squarely in the multifaceted landscape of factors regulating oligodendrocyte differentiation. A primary role for Klk6 as part of an oligodendrocyte-derived regulatory network can be readily envisioned. Klk6 secreted by OPCs or more mature oligodendrocytes is positioned to feedback in an autocrine, or feed forward in a paracrine manner, to cleave thereby activating oligodendrocyte PAR1 and/or PAR2. Klk6 is upregulated developmentally to become densely expressed by oligodendrocytes in adulthood and therefore can operate through autocrine or paracrine mechanisms to limit further myelin production. Additional efforts are needed to identify the oligodendrocyte-specific roles of Klk6 *in vivo*, which current studies suggest include a role as a negative regulator of extrinsic pro-myelinating signals such as BDNF, but other roles in the oligodendrocyte developmental program, or function in adulthood remain to be addressed. For example, Klk6 can cleave, thereby modifying, extracellular matrix molecules; this is an additional area where investigation of the actions of Klk6 in myelin development would be warranted. Since Klk6 is upregulated by astrocytes and infiltrating immune cells in the context of CNS injury and disease, including MS lesions and experimental models of MS, additional efforts to understand how blocking Klk6 improves outcomes, as suggested by

both our prior studies (Blaber et al. 2004; Scarisbrick et al. 2012b) and more recent studies (Bando et al. 2018), including through a mechanism that can unleash myelin regeneration, will be of high clinical relevance.

Acknowledgements:

Studies were supported by the National Institutes of Health R01NS052741–10, Pilot Project G-1510–06548 and Research Grants (G-1508–05951, RG-1901–33209) from the National Multiple Sclerosis Society and the Mayo Clinic Center for MS and Autoimmune Neurology (IAS). Support from the Cooperation Program in Cancer Research of the German Cancer Research Center (DKFZ) and Israel's Ministry of Science, Technology and Space (MOST) (Grant GR-2495 to A.K.M) is also acknowledged. ET was supported by the National Institute of General Medical Sciences (T32 GM 65841). The authors also thank Dr. G. Sotiropoulou for generously providing the Klk6 knockout mice.

References

Angelo PF, Lima AR, Alves FM, Blaber SI, Scarisbrick IA, Blaber M, Juliano L, Juliano MA. 2006. Substrate specificity of human kallikrein 6: salt and glycosaminoglycan activation effects. J Biol Chem 281:3116–26. [PubMed: 16321973]

Anisowicz A, Sotiropoulou G, Stenman G, Mok SC, Sager R. 1996. A novel protease homolog differentially expressed in breast and ovarian cancer. Mol Med 2:624–36. [PubMed: 8898378]

Bando Y, Hagiwara Y, Suzuki Y, Yoshida K, Aburakawa Y, Kimura T, Murakami C, Ono M, Tanaka T, Jiang YP and others. 2018. Kallikrein 6 secreted by oligodendrocytes regulates the progression of experimental autoimmune encephalomyelitis. Glia 66:359–378. [PubMed: 29086442]

Bando Y, Ito S, Nagai Y, Terayama R, Kishibe M, Jiang YP, Mitrovic B, Takahashi T, Yoshida S. 2006. Implications of protease M/neurosin in myelination during experimental demyelination and remyelination. Neurosci Lett 405:175–80. [PubMed: 16890353]

Bergles DE, Richardson WD. 2015. Oligodendrocyte Development and Plasticity. Cold Spring Harb Perspect Biol 8:a020453. [PubMed: 26492571]

Bernett MJ, Blaber SI, Scarisbrick IA, Dhanarajan P, Thompson SM, Blaber M. 2002. Crystal structure and biochemical characterization of human kallikrein 6 reveals that a trypsin-like kallikrein is expressed in the central nervous system. J Biol Chem 277:24562–70. [PubMed: 11983703]

Blaber SI, Ciric B, Christophi GP, Bernett MJ, Blaber M, Rodriguez M, Scarisbrick IA. 2004. Targeting kallikrein 6-proteolysis attenuates CNS inflammatory disease. FASEB J 19:920–922.

Blaber SI, Scarisbrick IA, Bernett MJ, Dhanarajan P, Seavy MA, Jin Y, Schwartz MA, Rodriguez M, Blaber M. 2002. Enzymatic properties of rat myelencephalon-specific protease. Biochemistry 41:1165–73. [PubMed: 11802715]

Blachnio-Zabielska AU, Persson XM, Koutsari C, Zabielski P, Jensen MD. 2012. A liquid chromatography/tandem mass spectrometry method for measuring the in vivo incorporation of plasma free fatty acids into intramyocellular ceramides in humans. Rapid Commun Mass Spectrom 26:1134–40. [PubMed: 22467464]

Boutin M, Sun Y, Shacka JJ, Auray-Blais C. 2016. Tandem Mass Spectrometry Multiplex Analysis of Glucosylceramide and Galactosylceramide Isoforms in Brain Tissues at Different Stages of Parkinson Disease. Anal Chem 88:1856–63. [PubMed: 26735924]

Bujalka H, Koenning M, Jackson S, Perreau VM, Pope B, Hay CM, Mitew S, Hill AF, Lu QR, Wegner M and others. 2013. MYRF is a membrane-associated transcription factor that autoproteolytically cleaves to directly activate myelin genes. PLoS Biol 11:e1001625. [PubMed: 23966833]

Burda JE, Radulovic M, Yoon H, Scarisbrick IA. 2013. Critical role for PAR1 in kallikrein 6-mediated oligodendrogliopathy. Glia 61:1456–70. [PubMed: 23832758]

Cahoy JD, Emery B, Kaushal A, Foo LC, Zamanian JL, Christopherson KS, Xing Y, Lubischer JL, Krieg PA, Krupenko SA and others. 2008. A transcriptome database for astrocytes, neurons, and oligodendrocytes: a new resource for understanding brain development and function. J Neurosci 28:264–78. [PubMed: 18171944]

Chrast R, Saher G, Nave KA, Verheijen MH. 2011. Lipid metabolism in myelinating glial cells: lessons from human inherited disorders and mouse models. J Lipid Res 52:419–34. [PubMed: 21062955]

Czopka T, von Holst A, ffrench-Constant C, Faissner A. 2010. Regulatory mechanisms that mediate tenascin C-dependent inhibition of oligodendrocyte precursor differentiation. J Neurosci 30:12310–22. [PubMed: 20844127]

De Vita E, Schuler P, Lovell S, Lohbeck J, Kullmann S, Rabinovich E, Sananes A, Hessling B, Hamon V, Papo N and others. 2018. Depsipeptides Featuring a Neutral P1 Are Potent Inhibitors of Kallikrein-Related Peptidase 6 with On-Target Cellular Activity. J Med Chem 61:8859–8874. [PubMed: 30212625]

De Vita E, Smits N, van den Hurk H, Beck EM, Hewitt J, Baillie G, Russell E, Pannifer A, Hamon V, Morrison Aand others. 2020. Synthesis and Structure-Activity Relationships of N-(4-Benzamidino)-Oxazolidinones: Potent and Selective Inhibitors of Kallikrein-Related Peptidase 6. ChemMedChem 15:79–95. [PubMed: 31675166]

Dick KJ, Eckhardt M, Paisan-Ruiz C, Alshehhi AA, Proukakis C, Sibtain NA, Maier H, Sharifi R, Patton MA, Bashir W and others. 2010. Mutation of FA2H underlies a complicated form of hereditary spastic paraplegia (SPG35). Hum Mutat 31:E1251–60. [PubMed: 20104589]

Dyer CA, Benjamins JA. 1989. Organization of oligodendroglial membrane sheets: II. Galactocerebroside:antibody interactions signal changes in cytoskeleton and myelin basic protein. J Neurosci Res 24:212–21. [PubMed: 2479764]

Elbaz B, Popko B. 2019. Molecular Control of Oligodendrocyte Development. Trends Neurosci 42:263–277. [PubMed: 30770136]

Emery B, Lu QR. 2015. Transcriptional and Epigenetic Regulation of Oligodendrocyte Development and Myelination in the Central Nervous System. Cold Spring Harb Perspect Biol 7:a020461. [PubMed: 26134004]

Fletcher JL, Wood RJ, Nguyen J, Norman EML, Jun CMK, Prawdiuk AR, Biemond M, Nguyen HTH, Northfield SE, Hughes RAand others. 2018. Targeting TrkB with a Brain-Derived Neurotrophic Factor Mimetic Promotes Myelin Repair in the Brain. J Neurosci 38:7088–7099. [PubMed: 29976621]

Fulmer CG, VonDran MW, Stillman AA, Huang Y, Hempstead BL, Dreyfus CF. 2014. Astrocyte-derived BDNF supports myelin protein synthesis after cuprizone-induced demyelination. J Neurosci 34:8186–96. [PubMed: 24920623]

Furusho M, Dupree JL, Nave KA, Bansal R. 2012. Fibroblast growth factor receptor signaling in oligodendrocytes regulates myelin sheath thickness. The Journal of neuroscience : the official journal of the Society for Neuroscience 32:6631–41. [PubMed: 22573685]

Fyffe-Maricich SL, Schott A, Karl M, Krasno J, Miller RH. 2013. Signaling through ERK1/2 controls myelin thickness during myelin repair in the adult central nervous system. J Neurosci 33:18402–8. [PubMed: 24259565]

Guardiola-Diaz HM, Ishii A, Bansal R. 2012. Erk1/2 MAPK and mTOR signaling sequentially regulates progression through distinct stages of oligodendrocyte differentiation. Glia 60:476–86. [PubMed: 22144101]

Harrington EP, Zhao C, Fancy SP, Kaing S, Franklin RJ, Rowitch DH. 2010. Oligodendrocyte PTEN is required for myelin and axonal integrity, not remyelination. Annals of neurology 68:703–16. [PubMed: 20853437]

Hebb AL, Bhan V, Wishart AD, Moore CS, Robertson GS. 2011. Human kallikrein 6 cerebrospinal levels are elevated in multiple sclerosis. Curr Drug Discov Technol 7:137–40.

Ishii A, Furusho M, Bansal R. 2013. Sustained activation of ERK1/2 MAPK in oligodendrocytes and schwann cells enhances myelin growth and stimulates oligodendrocyte progenitor expansion. J Neurosci 33:175–86. [PubMed: 23283332]

Ishii A, Fyffe-Maricich SL, Furusho M, Miller RH, Bansal R. 2012. ERK1/ERK2 MAPK signaling is required to increase myelin thickness independent of oligodendrocyte differentiation and initiation of myelination. J Neurosci 32:8855–64. [PubMed: 22745486]

Ligon KL, Fancy SP, Franklin RJ, Rowitch DH. 2006. Olig gene function in CNS development and disease. Glia 54:1–10. [PubMed: 16652341]

Little SP, Dixon EP, Norris F, Buckley W, Becker GW, Johnson M, Dobbins JR, Wyrick T, Miller JR, MacKellar W and others. 1997. Zyme, a novel and potentially amyloidogenic enzyme cDNA isolated from Alzheimer's disease brain. J Biol Chem 272:25135–42. [PubMed: 9312124]

Murakami K, Jiang YP, Tanaka T, Bando Y, Mitrovic B, Yoshida S. 2013. In vivo analysis of kallikrein-related peptidase 6 (KLK6) function in oligodendrocyte development and the expression of myelin proteins. Neuroscience 236:1–11. [PubMed: 23376368]

Narayanan SP, Flores AI, Wang F, Macklin WB. 2009. Akt signals through the mammalian target of rapamycin pathway to regulate CNS myelination. J Neurosci 29:6860–70. [PubMed: 19474313]

Norton WT, Poduslo SE. 1973. Myelination in rat brain: method of myelin isolation. J Neurochem 21:749–57. [PubMed: 4271082]

Oikonomopoulou K, Hansen KK, Saifeddine M, Tea I, Blaber M, Blaber SI, Scarisbrick I, Andrade-Gordon P, Cottrell GS, Bunnett NW and others. 2006. Proteinase-activated receptors, targets for kallikrein signaling. J Biol Chem 281:32095–112. [PubMed: 16885167]

Paik MJ, Yu J, Hu MB, Kim SJ, Kim KR, Ahn YH, Choi S, Lee G. 2008. Gas chromatographic-mass spectrometric analyses of cholesterol and its precursors in rat plasma as tert-butyldimethylsilyl derivatives. Clin Chim Acta 396:62–5. [PubMed: 18657530]

Pampalakis G, Sykioti VS, Ximerakis M, Stefanakou-Kalakou I, Melki R, Vekrellis K, Sotiropoulou G. 2017. KLK6 proteolysis is implicated in the turnover and uptake of extracellular alpha-synuclein species. Oncotarget 8:14502–14515. [PubMed: 27845893]

Panos M, Christophi GP, Rodriguez M, Scarisbrick IA. 2014. Differential expression of multiple kallikreins in a viral model of multiple sclerosis points to unique roles in the innate and adaptive immune response. Biol Chem 395:1063–73. [PubMed: 25153387]

Radulovic M, Yoon H, Larson N, Wu J, Linbo R, Burda JE, Diamandis EP, Blaber SI, Blaber M, Fehlings MG and others. 2013. Kallikrein cascades in traumatic spinal cord injury: in vitro evidence for roles in axonopathy and neuron degeneration. Journal of neuropathology and experimental neurology 72:1072–89. [PubMed: 24128681]

Radulovic M, Yoon H, Wu J, Mustafa K, Scarisbrick IA. 2016. Targeting the thrombin receptor modulates inflammation and astrogliosis to improve recovery after spinal cord injury. Neurobiol Dis 93:226–42. [PubMed: 27145117]

Ramos-Cejudo J, Gutierrez-Fernandez M, Otero-Ortega L, Rodriguez-Frutos B, Fuentes B, Vallejo-Cremades MT, Hernanz TN, Cerdan S, Diez-Tejedor E. 2015. Brain-derived neurotrophic factor administration mediated oligodendrocyte differentiation and myelin formation in subcortical ischemic stroke. Stroke 46:221–8. [PubMed: 25395417]

Samantha Sykioti V, Karampetsou M, Chalatsa I, Polissidis A, Michael IP, Pagaki-Skaliora M, Nagy A, Emmanouilidou E, Sotiropoulou G, Vekrelli SK. 2020. Deficiency of the serine peptidase Kallikrein 6 does not affect the levels and the pathological accumulation of a-synuclein in mouse brain. J Neurochem.

Scarisbrick IA, Asakura K, Blaber S, Blaber M, Isackson PJ, Bieto T, Rodriguez M, Windebank AJ. 2000. Preferential expression of myelencephalon-specific protease by oligodendrocytes of the adult rat spinal cord white matter. Glia 30:219–30. [PubMed: 10756072]

Scarisbrick IA, Blaber M. 2012. Kallikrein-related peptidase 6. In: Barrett AJ, Rawlings ND, editors. Handbook of Proteolytic Enzymes. London, UK: Elsevier. p 2780–2786.

Scarisbrick IA, Blaber SI, Lucchinetti CF, Genain CP, Blaber M, Rodriguez M. 2002. Activity of a newly identified serine protease in CNS demyelination. Brain 125:1283–96. [PubMed: 12023317]

Scarisbrick IA, Blaber SI, Tingling JT, Rodriguez M, Blaber M, Christophi GP. 2006a. Potential scope of action of tissue kallikreins in CNS immune-mediated disease. J Neuroimmunol 178:167–76. [PubMed: 16824622]

Scarisbrick IA, Epstein B, Cloud BA, Yoon H, Wu J, Renner DN, Blaber SI, Blaber M, Vandell AG, Bryson AL. 2011. Functional role of kallikrein 6 in regulating immune cell survival. PLoS One 6:e18376; 1–11.

Scarisbrick IA, Isackson PJ, Ciric B, Windebank AJ, Rodriguez M. 2001. MSP, a trypsin-like serine protease, is abundantly expressed in the human nervous system. J Comp Neurol 431:347–61. [PubMed: 11170010]

Scarisbrick IA, Linbo R, Vandell AG, Keegan M, Blaber SI, Blaber M, Sneve D, Lucchinetti CF, Rodriguez M, Diamandis EP. 2008. Kallikreins are associated with secondary progressive multiple sclerosis and promote neurodegeneration. Biol Chem 389:739–45. [PubMed: 18627300]

Scarisbrick IA, Radulovic M, Burda JE, Larson N, Blaber SI, Giannini C, Blaber M, Vandell AG. 2012a. Kallikrein 6 is a novel molecular trigger of reactive astrogliosis. Biological Chemistry 393:355–67. [PubMed: 22505518]

Scarisbrick IA, Sabharwal P, Cruz H, Larsen N, Vandell A, Blaber SI, Ameenuddin S, Papke LM, Fehlings MG, Reeves RK and others. 2006b. Dynamic role of kallikrein 6 in traumatic spinal cord injury. Eur J Neuroscience 24:1457–1469.

Scarisbrick IA, Towner MD, Isackson PJ. 1997a. Nervous system specific expression of a novel serine protease: regulation in the adult rat spinal cord by excitotoxic injury. The Journal of neuroscience : the official journal of the Society for Neuroscience 17:8156–8168. [PubMed: 9334391]

Scarisbrick IA, Towner MD, Isackson PJ. 1997b. Nervous system-specific expression of a novel serine protease: regulation in the adult rat spinal cord by excitotoxic injury. J Neurosci 17:8156–68. [PubMed: 9334391]

Scarisbrick IA, Yoon H, Panos M, Larson N, Blaber SI, Blaber M, Rodriguez M. 2012b. Kallikrein 6 regulates early CNS demyelination in a viral model of multiple sclerosis. Brain Pathol 22:709–22. [PubMed: 22335454]

Schutzer SE, Angel TE, Liu T, Schepmoes AA, Xie F, Bergquist J, Vecsei L, Zadori D, Camp DG 2nd, Holland BK and others. 2013. Gray matter is targeted in first-attack multiple sclerosis. PLoS One 8:e66117. [PubMed: 24039694]

Singh V, van Pelt ED, Stoop MP, Stingl C, Ketelslegers IA, Neuteboom RF, Catsman-Berrevoets CE, Luider TM, Hintzen RQ. 2015. Gray matter-related proteins are associated with childhood-onset multiple sclerosis. Neurol Neuroimmunol Neuroinflamm 2:e155. [PubMed: 26445729]

Stassart RM, Mobius W, Nave KA, Edgar JM. 2018. The Axon-Myelin Unit in Development and Degenerative Disease. Front Neurosci 12:467. [PubMed: 30050403]

Uchida A, Oka Y, Aoyama M, Suzuki S, Yokoi T, Katano H, Mase M, Tada T, Asai K, Yamada K. 2004. Expression of myelencephalon-specific protease in transient middle cerebral artery occlusion model of rat brain. Brain Res Mol Brain Res 126:129–36. [PubMed: 15249136]

Vandell AG, Larson N, Laxmikanthan G, Panos M, Blaber SI, Blaber M, Scarisbrick IA. 2008. Protease Activated Receptor Dependent and Independent Signaling by Kallikreins 1 and 6 in CNS Neuron and Astroglial Cell Lines. J Neurochem 107:855–870. [PubMed: 18778305]

VonDran MW, Singh H, Honeywell JZ, Dreyfus CF. 2011. Levels of BDNF impact oligodendrocyte lineage cells following a cuprizone lesion. J Neurosci 31:14182–90. [PubMed: 21976503]

Wang J, Lu QR. 2020. Convergent epigenetic regulation of glial plasticity in myelin repair and brain tumorigenesis: A focus on histone modifying enzymes. Neurobiol Dis 144:105040. [PubMed: 32800999]

Wong AW, Xiao J, Kemper D, Kilpatrick TJ, Murray SS. 2013. Oligodendroglial expression of TrkB independently regulates myelination and progenitor cell proliferation. J Neurosci 33:4947–57. [PubMed: 23486965]

Yamanaka H, He X, Matsumoto K, Shiosaka S, Yoshida S. 1999. Protease M/neurosin mRNA is expressed in mature oligodendrocytes. Brain Res Mol Brain Res 71:217–24. [PubMed: 10521576]

Yamashiro K, Tsuruoka N, Kodama S, Tsujimoto M, Yamamura Y, Tanaka T, Nakazato H, Yamaguchi N. 1997. Molecular cloning of a novel trypsin-like serine protease (neurosin) preferentially expressed in brain. Biochim Biophys Acta 1350:11–4. [PubMed: 9003450]

Yeung MSY, Djelloul M, Steiner E, Bernard S, Salehpour M, Possnert G, Brundin L, Frisen J. 2019. Dynamics of oligodendrocyte generation in multiple sclerosis. Nature 566:538–542. [PubMed: 30675058]

Yoon H, Choi CI, Triplet EM, Langley MR, Kleppe LS, Kim HN, Simon WL, Scarisbrick IA. 2020. Blocking the Thrombin Receptor Promotes Repair of Demyelinated Lesions in the Adult Brain. J Neurosci 40:1483–1500. [PubMed: 31911460]

Yoon H, Radulovic M, Drucker KL, Wu J, Scarisbrick IA. 2015. The thrombin receptor is a critical extracellular switch controlling myelination. Glia 63:846–59. [PubMed: 25628003]

Yoon H, Radulovic M, Scarisbrick IA. 2018. Kallikrein-related peptidase 6 orchestrates astrocyte form and function through proteinase activated receptor-dependent mechanisms. Biol Chem 399:1041–1052. [PubMed: 29604205]

Yoon H, Radulovic M, Walters G, Paulsen AR, Drucker K, Starski P, Wu J, Fairlie DP, Scarisbrick IA. 2017. Protease activated receptor 2 controls myelin development, resiliency and repair. Glia 65:2070–2086. [PubMed: 28921694]

Yoon H, Radulovic M, Wu J, Blaber SI, Blaber M, Fehlings MG, Scarisbrick IA. 2013. Kallikrein 6 signals through PAR1 and PAR2 to promote neuron injury and exacerbate glutamate neurotoxicity. J Neurochem 127:283–98. [PubMed: 23647384]

Yoon H, Scarisbrick IA. 2016. Kallikrein-related peptidase 6 exacerbates disease in an autoimmune model of multiple sclerosis. Biol Chem 397:1277–1286. [PubMed: 27533119]

Highlights

- Klk6 gene knockout accelerates developmental myelination.
- Genetic or pharmacologic inhibition of Klk6 in OPCs enhances differentiation.
- An interplay between Klk6 inhibition and BDNF augments oligodendrocyte differentiation.

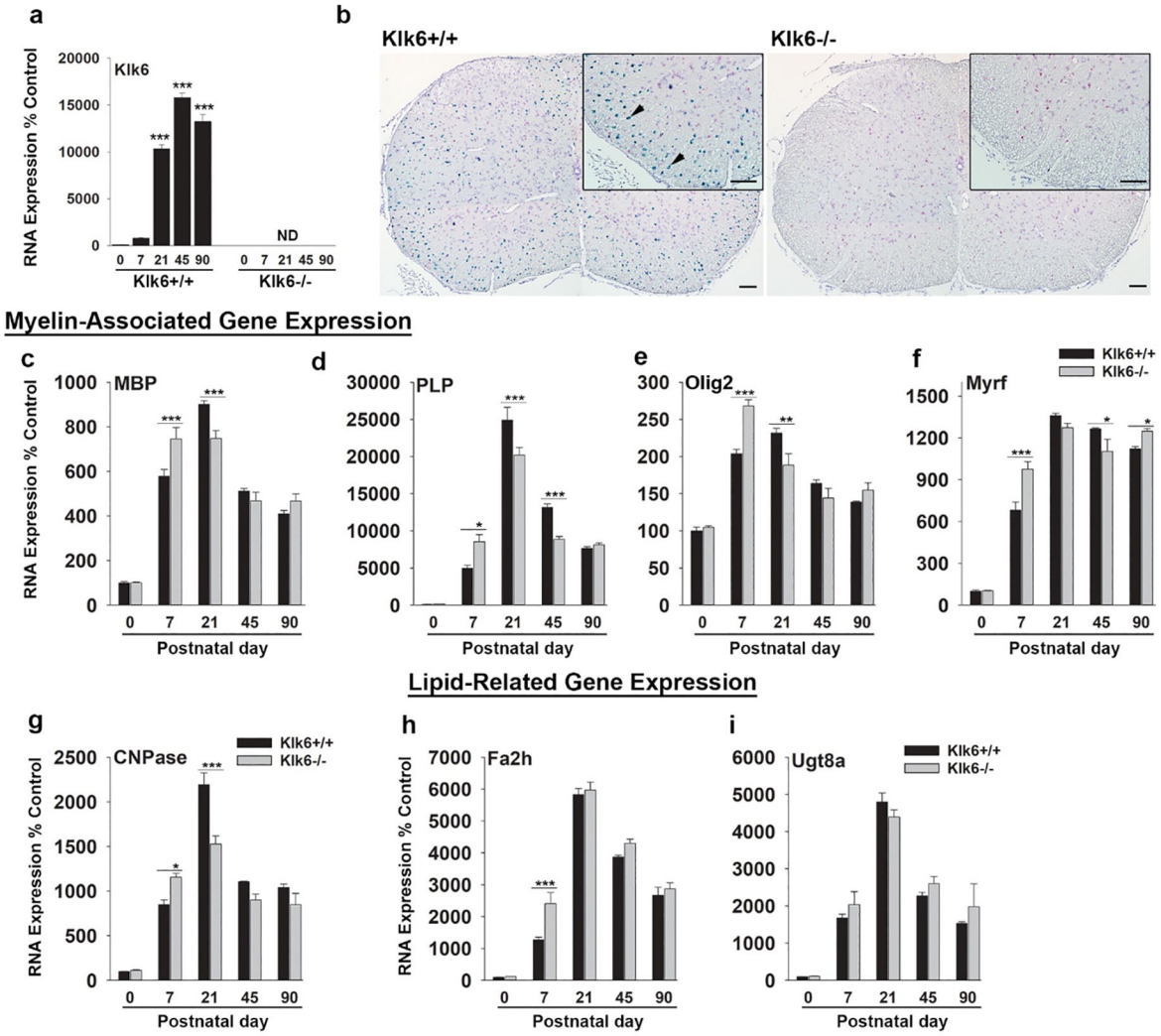

Figure 1. Klk6 gene knockout results in accelerated expression of myelin and lipid synthesis genes.

(a) Histogram shows developmental time course of Klk6 RNA expression detected by real time PCR in the murine spinal cord which is very low at birth and reaches a peak at P21. (b) Photomicrographs show *in situ* hybridization for Klk6 RNA in the spinal cord of Klk6+/+ and Klk6−/− mice (arrows point to a selection of Klk6-expressing cells, sections were counterstained with hematoxylin). Klk6 RNA expression was not detected (ND) in Klk6−/− knockouts. (c-i) Histograms show expression of myelin-associated (*Mbp*, *Plp*, *Olig2*, *Myrf*, *CNPase*) and lipid-related (*Fa2h* and *Ugt8a*) genes in the spinal cord of Klk6+/+ and Klk6−/− mice from P0 to P90, with higher levels in knockouts by P7 ($P \leq 0.001$, n = 3, male and female mice per time point). Statistical evaluations in c-i were done by one-way ANOVA followed by NK post hoc test. Asterisks represent significant differences with *$P < 0.05$; **$P < 0.01$; ***$P \leq 0.001$. Scale bar in (a) indicates 100 μm.

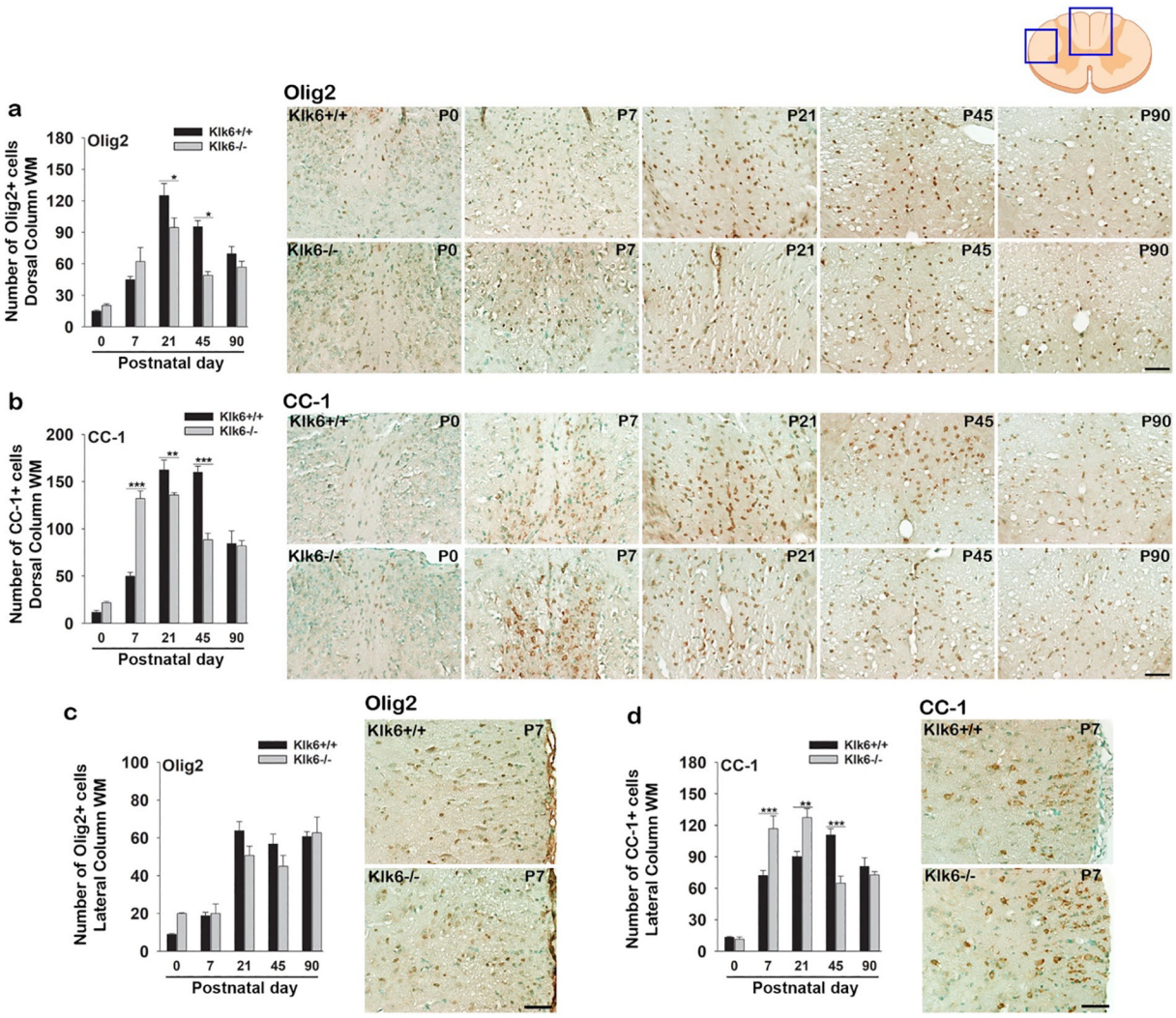

Figure 2. Klk6 gene knockout results in accelerated oligodendrocyte maturation.

Histograms and associated photomicrographs (a-d) show counts of Olig2+ and CC-1 positive oligodendrocytes in the spinal cord dorsal columns (a, b) or in the ventrolateral white matter (c, d) from P0 to P90. Counts of oligodendrocytes positive for CC-1, a marker of mature oligodendrocytes, were greater at P7 in Klk6−/− compared to Klk6+/+. After P7, numbers of Olig2 and CC-1 positive oligodendrocytes trended to being reduced in Klk6-/−. (*P < 0.05; **P < 0.01; ***P ≤ 0.001, n = 3–4, male and female mice per time point). Statistical evaluations in c-d were accomplished by One-way ANOVA followed by NK post hoc test. Scale bars indicate 50 μm.

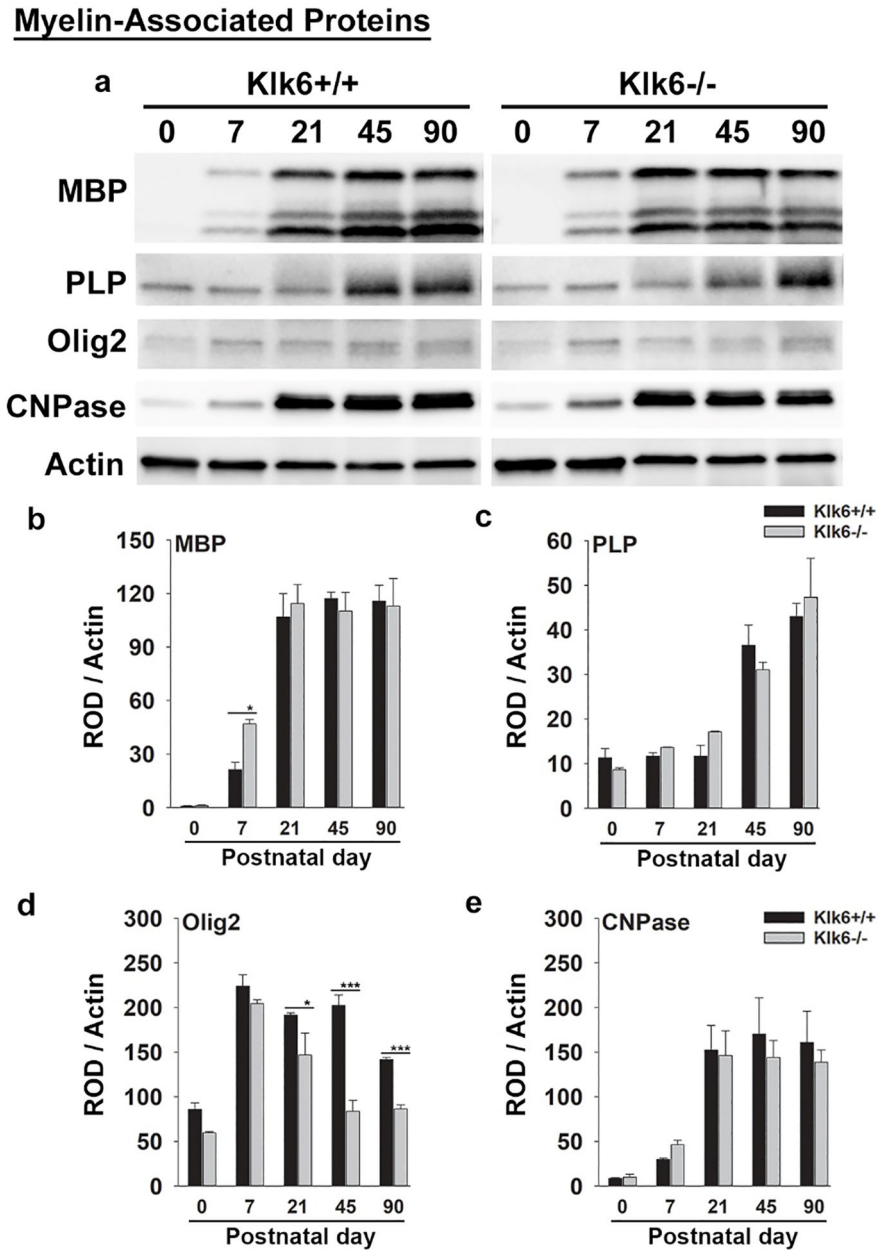

Figure 3. Accelerated developmental expression of myelin basic protein in the spinal cord of Klk6 gene knockout mice.

Western blots of whole spinal cord homogenates and associated histograms (a-e) illustrate that mice lacking Klk6 show significant increases in MBP at P7. No significant differences in PLP or CNPase were observed, but levels of Olig2 were reduced by P21 and at P90. (*P < 0.05; **P < 0.01; ***P ≤ 0.001, n = 3, male and female mice). Statistical evaluations in a-e were done by one-way ANOVA followed by NK post hoc test.

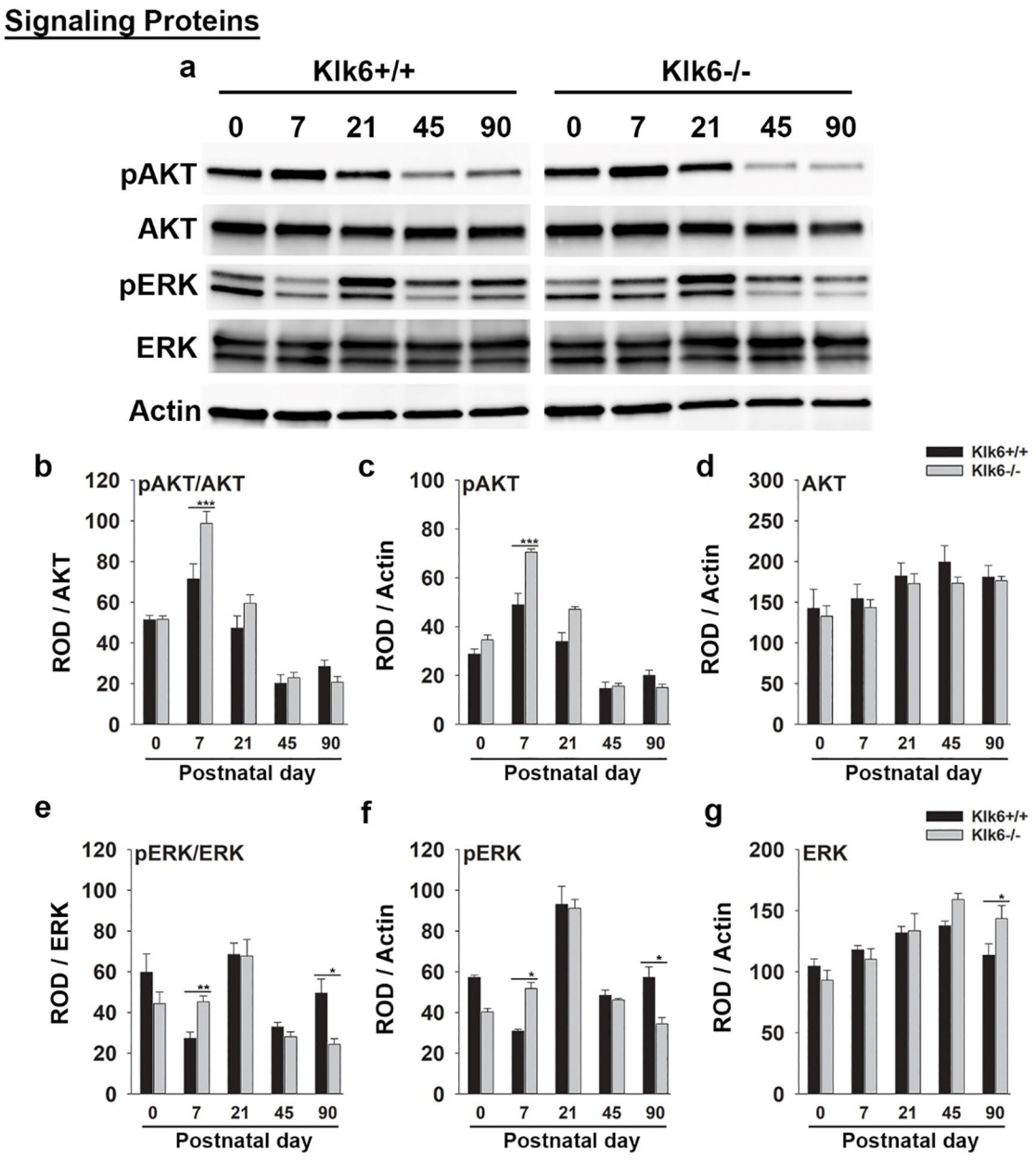

Figure 4. Accelerated developmental AKT and ERK1/2 signaling in the spinal cord of Klk6 gene knockout mice.

Western blots of whole spinal cord homogenates and associated histograms (a-g) illustrate that Klk6 gene knockout mice show significant increases in AKT and ERK1/2 signaling at P7, with overall ERK1/2 signaling reduced by P90. (*P < 0.05; **P < 0.01; ***P ≤ 0.001, n = 3, male and female mice). Statistical evaluations in b-g were done by one-way ANOVA followed by NK post hoc test.

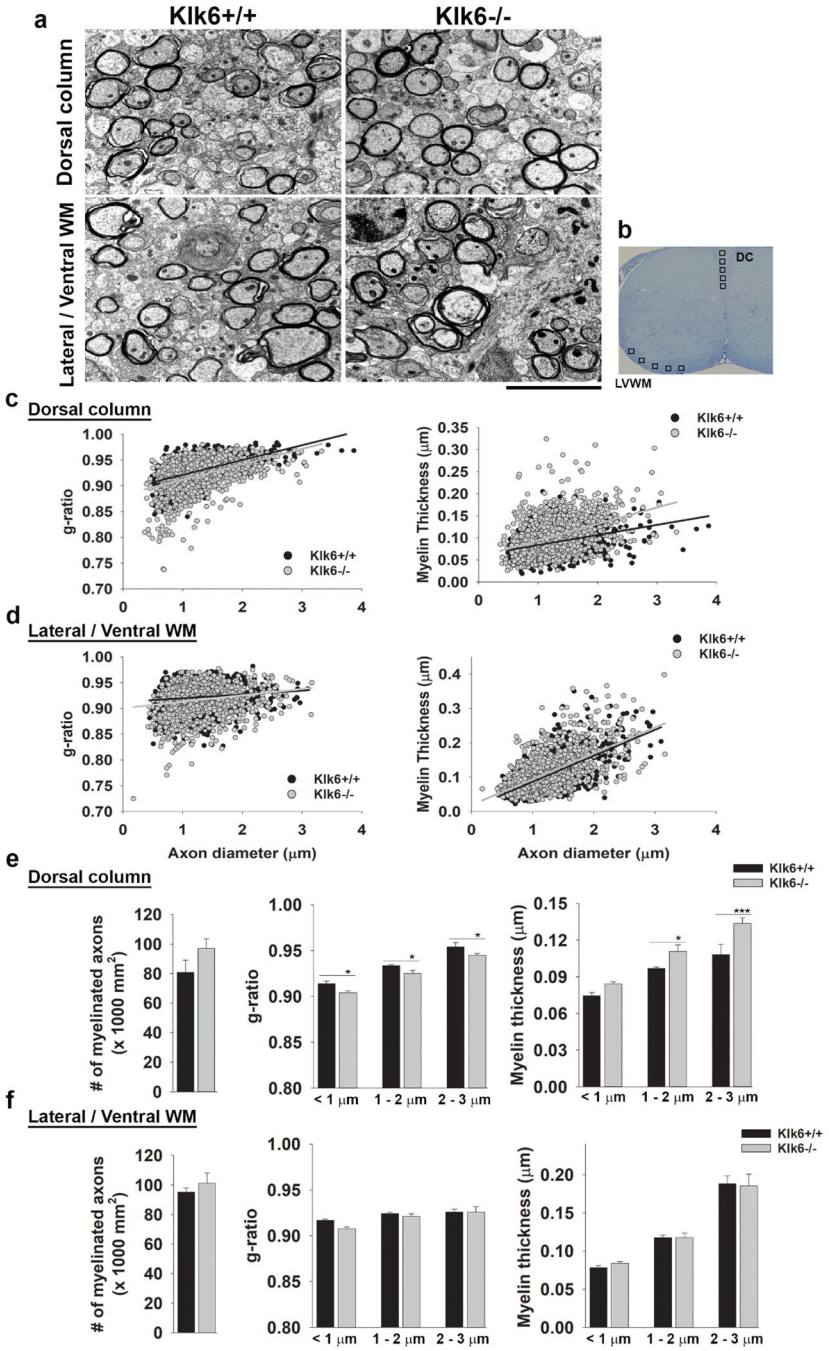

Figure 5. Klk6 gene knockout results in increases in myelin thickness in the P7 spinal cord.

(a) Representative electron micrographs taken from the spinal cord dorsal columns or ventral lateral white matter of P7 Klk6+/+ or Klk6−/− mice (areas sampled are boxed in (b)). Micrographs were used to enumerate the number of myelinated axons and to calculate g-ratios and myelin thickness. G-ratios are plotted relative to axon diameter at P7 (c and d). Histograms show the mean g-ratios and myelin thickness for axons across a range of diameters (e and f). In dorsal column white matter (e), mean g-ratios across all axons were significantly lower in Klk6−/− mice compared with Klk6+/+ (< 1 μm, P = 0.02, 1–2 μm, P =

0.046 and 2–3 μm, P = 0.03). Mean myelin thickness was significantly greater in Klk6−/− in association with axon diameters < 1 μm (1–2 μm, P = 0.05 and 2–3 μm, P < 0.001). (f) The number of myelinated axons was not significantly increased in mice lacking Klk6. P < 0.05; **P < 0.01; ***P ≤ 0.001). Statistical evaluations were done by two-way ANOVA followed by NK post hoc test or Student's t-test, n = 3 female and 4 male mice per genotype. Scale bars in a indicate 5 μm.

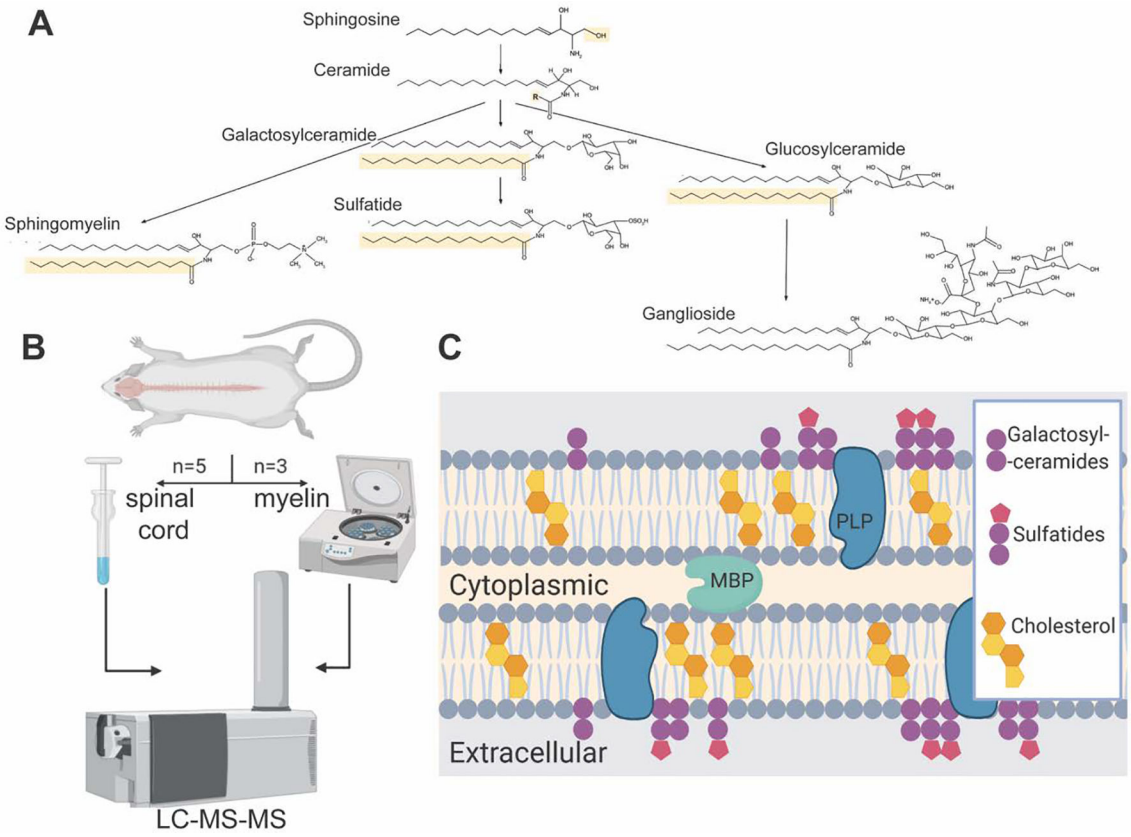

Figure 6. Overview of primary CNS lipid synthesis intermediates and experimental procedure for quantification of lipid species.

(a) Schematic shows sequential lipid species in the synthesis pathways, starting with addition of a fatty acid side chain (“R”) to a sphingosine backbone to form ceramides. Ceramides can be modified by addition of choline phosphate, galactose, and glucose head groups to form the major classes of sphingomyelins, sulfatides, and gangliosides, respectively. (b) Lipids in whole spinal cord or in purified myelin were quantified by LC-MS/MS (see Tables 2 and 3). (c) Cartoon shows key lipid and protein constituents of the myelin membrane, with galactosylceramides and sulfatides found almost exclusively on the extracellular membrane layer and frequently forming lipid raft microdomains along with cholesterol in which key structural proteins, including PLP, are clustered (Dyer and Benjamins 1989).

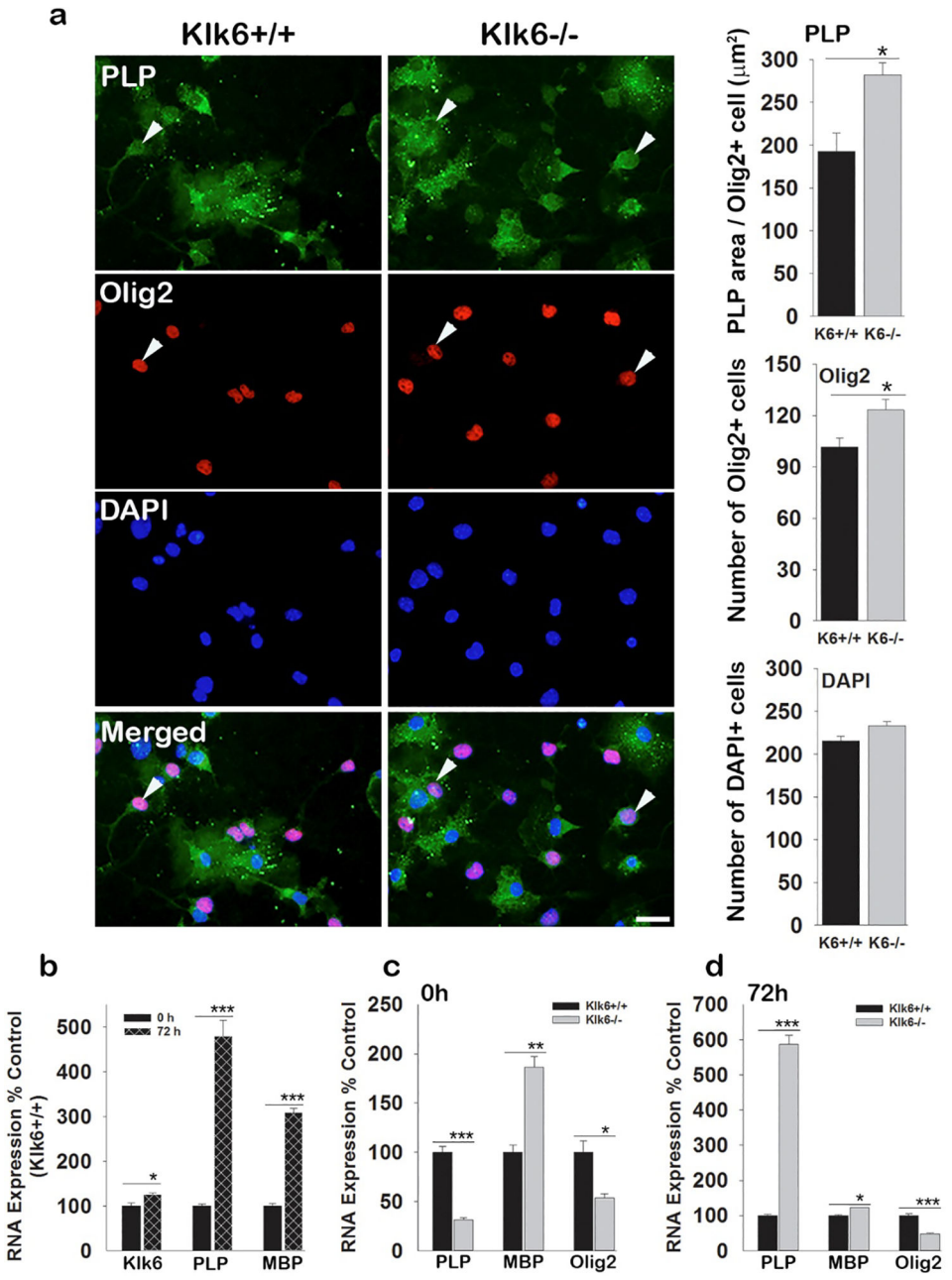

Figure 7. Oligodendrocyte progenitors with Klk6 gene knockout express higher levels of PLP at early stages of differentiation *in vitro*.

(a) Photomicrographs and associated histograms demonstrate Klk6−/− OPC cultures show greater PLP area /Olig2+ cells and greater numbers of Olig2+ cells after a 72 h period of differentiation. **(b)** Histogram shows real time PCR quantification of *Klk6*, *Plp* and *Mbp* RNA expression in wild type primary OPCs at 0 and 72 h after switching to oligodendrocyte differentiation media. The expected large increases in *Plp* and *Mbp* were observed in addition to smaller increases in *Klk6* RNA expression, over the same period. **(c, d)** Histograms show expression of *Plp*, *Mbp* and *Olig2* in OPCs differentiated *in vitro* for 0 or 72 h, with significantly higher levels of *Plp* and *Mbp* and lower *Olig2* in Klk6−/−

OPCs at 72 h compared to Klk6+/+. Statistical evaluation was done by Student's t test. Asterisks represent significant differences with *P < 0.05; **P < 0.01; ***P ≤ 0.001. Scale bar indicates 20 μm.

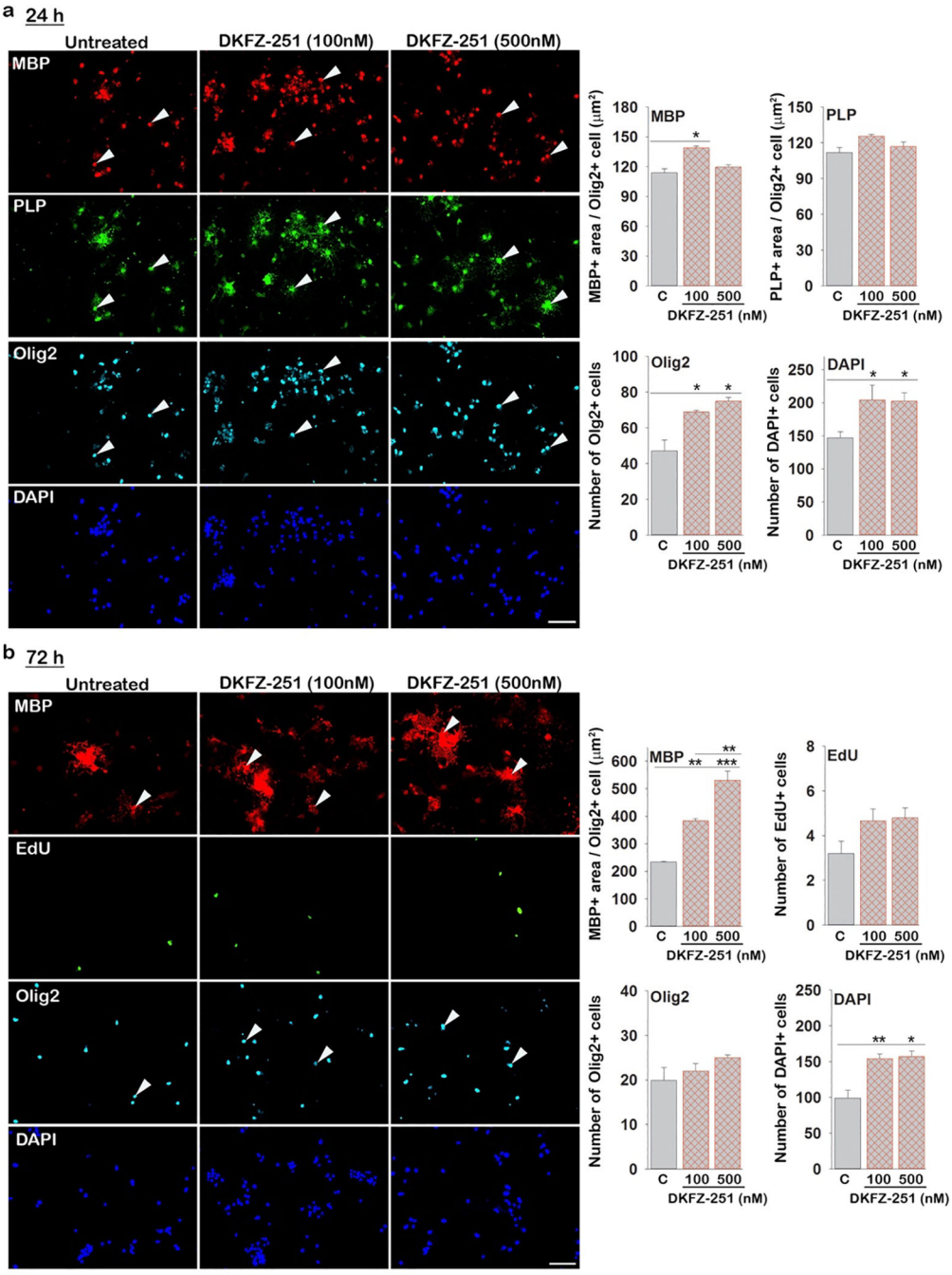

Figure 8. Pharmacologic inhibition of Klk6 increases MBP expression by oligodendrocyte progenitors *in vitro*.

Fluorescent images and associated histograms show changes in expression of myelin markers at (a) 24 or (b) 72 h after plating OPCs under differentiation conditions with the addition of a Klk6 small molecule inhibitor, DKFZ-251 (100 or 500 nM) or vehicle alone (DMSO). Inhibition of Klk6 during the early stages of OPC differentiation increased total MBP area/Olig2+ oligodendrocytes and the number of Olig2+ cells at 24 h. Inhibition of Klk6 resulted in a dose-dependent increase in MBP area/Olig2+ cells at 72 h. (*P < 0.05;

**P < 0.01; ***P ≤ 0.001). Statistical evaluations were done by One-way ANOVA followed by NK post hoc test. Scale bars in a and b indicate 50 μm.

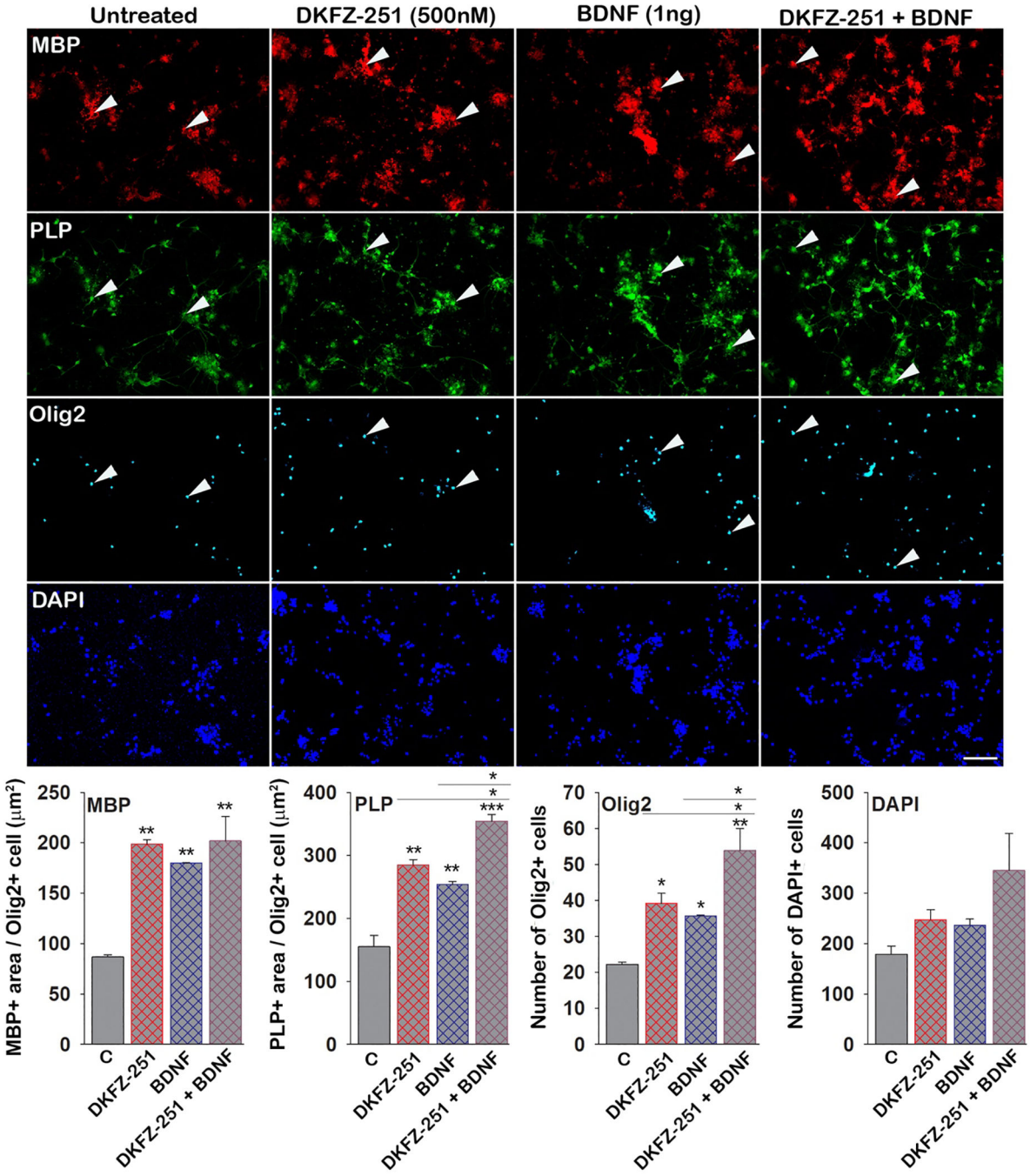

Figure 9. Interplay between Klk6 and brain derived neurotrophic factor regulate myelin protein production *in vitro*.

Fluorescent images and associated histograms show changes in expression of myelin markers at 72 h after plating OPCs under differentiation conditions with the addition of the Klk6 small molecule inhibitor, DKFZ-251 (500 nM), suboptimal levels of BDNF (1 ng/ml), a combination of DKFZ-251 + BDNF, or vehicle alone (DMSO, designated as C). Inhibition of Klk6 during the early period of OPC differentiation increased total MBP and PLP area/Olig2+ oligodendrocytes, and the number of Olig2+ cells to levels comparable to that of 1 ng/ml BDNF. The combination of Klk6 inhibition plus BDNF supplementation

promoted even greater increases in PLP area/Olig2+ oligodendrocytes and Olig2+ cell counts, compared to BDNF alone. (*P < 0.05; **P < 0.01; ***P ≤ 0.001). Statistical evaluations in b-g were done by one-way ANOVA followed by NK post hoc test. Scale bar indicates 100 μm.

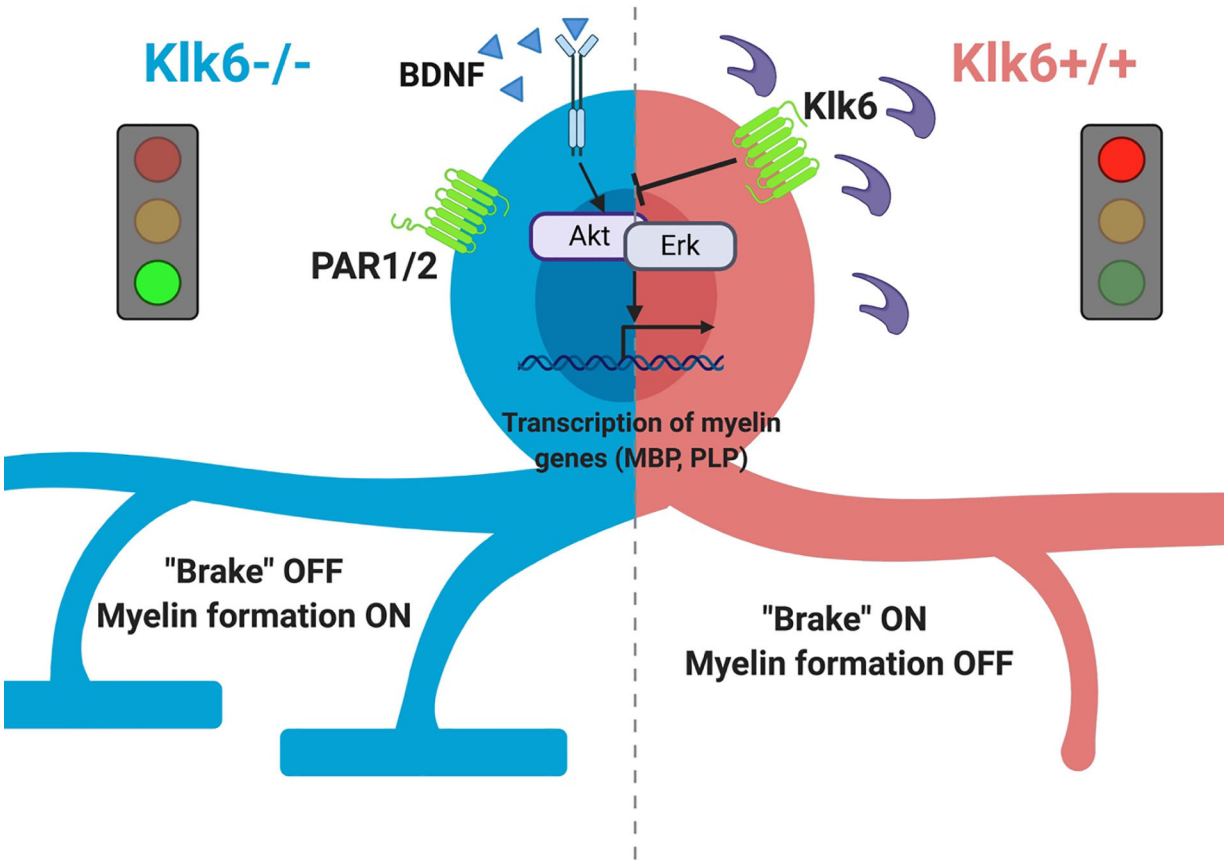

Figure 10. Working model depicting mechanism by which the level of Klk6 signaling regulates expression of MBP and PLP.

When CNS Klk6 levels are low, such as at birth, growth factors (for example BDNF) promote signaling in the AKT and ERK pathways, driving myelin production. As development proceeds, Klk6 expression progressively increases and this in turn activates PAR1 and PAR2 to suppress expression of myelin genes, for example MBP and PLP. In this model, the progressive increases in Klk6 expression that occurs until the P21 peak of myelination ultimately serve as a “brake” to limit additional myelin formation and therefore promote myelin homeostasis in adulthood.

Table 1.

Primers used for quantitative real-time PCR and genotyping.

Gene	Accession number	Probe and primer sets
Klk6	NM_011177.1	CCTACCCTGGCAAGATCA/GGATCCATCTGATATGAGTGC
CNPase	NM_001146318	CAAATTCTGTGACTACGGG/ GGCCTTGCCATACGA
Fa2h	NM_016967	Assay ID: Mm.PT.58.31646155
Olig2	NM_016967	Assay ID: Mm.PT.58.42319010
MBP	NM_001025251	CCAGTAGTCCATTTCTTCAAGAACAT/GCCGATTTATAGTCGGAAGCTC
PLP	NM_011123.2	TCTTTGGCGACTACAAGACCAC/CACAAACTTGTCGGGATGTCCTA
Myrf	NM_001033481.1	Assay ID: Mm01194959_m1 (Applied Biosystems)
Ugt8a	NM_011674	Assay ID: Mm.PT.58.8519332
Klk6 genotyping primers		
Mutant sense		AGTCAGGTCCTCTCTGTC
Mutant antisense		GATCCCCACTGGAAAGAC
Wild-type sense		AGTCAGGTCCTCTCTGTC
Wild-type antisense		TTCCCCAAGATCACCTGCAG

All probes and primers were obtained from Integrated DNA Technologies (IDT) unless otherwise indicated.

Table 2.

Whole spinal cord LC-MS-MS lipidomic profile

	P21				P90			
	Klk6+/+ Mean ± SEM	Klk6−/− Mean ± SEM	Fold change	p-value	Klk6+/+ Mean ± SEM	Klk6−/− Mean ± SEM	Fold change	p-value
Cholesterol (ng/mg tissue)								
Total	9.5 ± 0.76	12.7 ± 0.62	1.34	-	15.6 ± 0.45	15.3 ± 0.24	0.98	-
Free	8.3 ± 0.61	11.5 ± 0.52	1.38	**0.03**	14.6 ± 0.34	14.3 ± 0.21	0.98	-
Ceramides (ng/µg protein)								
Sph	1.5 ± 0.07	1.8 ± 0.05	1.26	**0.02**	2.3 ± 0.09	2.3 ± 0.09	1.00	-
SPA	0.88 ± 0.06	0.92 ± 0.06	1.04	-	0.53 ± 0.02	0.58 ± 0.04	1.08	-
S1P	6.3 ± 0.45	7.0 ± 1.10	1.12	-	17.3 ± 1.22	13.7 ± 0.31	0.79	-
C14_Cer	0.21 ± 0.03	0.19 ± 0.05	0.91	-	0.03 ± 9.90e-3	0.03 ± 2.07e-3	1.04	-
C16_Cer	1.5 ± 0.16	1.2 ± 0.12	0.81	-	1.1 ± 0.16	0.88 ± 0.05	0.83	-
C16dh_Cer	0.21 ± 0.04	0.18 ± 0.01	0.87	-	0.08 ± 0.03	0.10 ± 0.03	1.27	
C18_Cer	138.8 ± 10.44	137.8 ± 12.2	0.99	-	101.3 ± 5.87	101.4 ± 2.33	1.00	-
C18:1_Cer	0.28 ± 0.05	0.24 ± 0.03	0.86	-	0.05 ± 0.05	0.03 ± 0.02	0.61	-
C18dh_Cer	9.2 ± 1.09	9.8 ± 0.61	1.07		1.9 ± 0.26	2.1 ± 0.11	1.08	
C20_Cer	39.1 ± 2.09	40.0 ± 4.8	1.02	-	25.0 ± 2.23	27.4 ± 1.00	1.09	-
C22_Cer	47.8 ± 3.31	51.3 ± 7.59	1.07	-	41.4 ± 3.74	33.4 ± 0.61	0.81	-
C24_Cer	20.6 ± 1.38	21.8 ± 2.7	1.06	-	12.5 ± 1.18	10.3 ± 0.31	0.82	-
C24:1_Cer	88.2 ± 2.89	21.8 ± 2.73	1.04	-	88.3 ± 4.82	79.9 ± 1.65	0.90	-
Galactosylceramides (ng/µg protein)								
Gal_Sph	8.41e-4 ± 1.88e-3	0.00 ± 0.00	-	-	0.03 ± 5.63e-3	0.03 ± 5.20e-3	0.71	-
Gal_C16_Cer	0.36 ± 0.06	0.48 ± 0.05	1.31	-	0.52 ± 0.05	0.47 ± 0.05	0.91	-
Gal_C18_Cer	15.3 ± 1.75	20.2 ± 0.96	1.32	-	22.8 ± 1.34	18.9 ± 1.16	0.83	-
Gal_C20_Cer*	11.2 ± 1.27	14.2 ± 1.24	1.27	-	22.3 ± 2.60	21.0 ± 2.62	0.94	-
Gal_C22_Cer*	71.6 ± 12.58	93.6 ± 7.06	1.31	-	138.1 ± 3.26	117.1 ± 5.52	0.85	-
Gal_C24_Cer*	137.5 ± 24.60	177.8 ± 15.89	1.29	-	282.7 ± 14.45	247.9 ± 12.12	0.88	-
Gal_C24:1_Cer	60.5 ± 7.94	72.5 ± 7.04	1.20	-	101.3 ± 8.11	95.4 ± 6.09	0.94	-
Sphingomyelins (ng/µg protein)								
SM_C16	0.59 ± 0.03	0.94 ± 0.05	1.59	**0.01**	1.6 ± 0.04	1.3 ± 0.08	0.84	-
SM_C18:0	9.49 ± 1.38	13.4 ± 0.39	1.41	-	19.0 ± 1.14	19.5 ± 1.29	1.02	-
SM_C18:1	0.40 ± 0.07	0.49 ± 0.04	1.22	-	0.53 ± 0.04	0.55 ± 0.04	1.04	-
SM_C20:0*	2.45 ± 0.32	2.62 ± 0.17	1.07	-	4.4 ± 0.35	4.9 ± 0.14	1.12	-
SM_C22:0*	6.53 ± 0.78	6.28 ± 0.36	0.96	-	12.6 ± 0.95	15.1 ± 0.48	1.20	-
SM_C24:0	4.17 ± 0.52	4.56 ± 0.42	1.09	-	8.1 ± 0.45	10.6 ± 0.65	1.31	-

	P21				P90			
	Klk6+/+	Klk6−/−	Fold change	p-value	Klk6+/+	Klk6−/−	Fold change	p-value
	Mean ± SEM	Mean ± SEM			Mean ± SEM	Mean ± SEM		
SM_C24:1	13.1 ± 0.65	20.5 ± 1.42	1.56	**0.01**	42.8 ± 2.48	55.0 ± 3.32	1.28	-

Table shows quantification of lipid species and fold change of Klk6−/− relative to wild type (i.e. value >1 are species increased in Klk6−/−) in whole spinal cord from P21 or P90 female mice. Cholesterol levels were increased at the peak of myelination (P21) in Klk6−/− spinal cords with statistically significant increases in free (unesterified) cholesterol (P = 0.03). Most ceramides were equally abundant across time points between Klk6−/− and wild type spinal cords, with the exception of sphingosine, which is significantly enriched in Klk6−/− spinal cords at P21 (P = 0.02). Similarly, sphingomyelins tended to be more different during the peak of myelination, with statistically significant enrichment in both short (SM_C16) and long (SM_C24:1) chain sphingomyelins lessened by P90. Galactosylceramide abundance also changed through time, being more enriched in Klk6−/− spinal cords at P21, but less abundant compared to wild type by P90. N = 5 per genotype, per time point. All P values were adjusted for multiple comparisons with the Benjamini-Hochberg method with a false discovery rate of 0.05, significant P values in Table are bolded.

*Indicates lipid species which did not have a standard available; data was normalized by area ratio of analyte/internal standard.

Table 3

Myelin enriched fragment LC-MS-MS lipidomic profile

	P21				P90			
	Klk6+/+ Mean ± SEM	Klk6−/− Mean ± SEM	Fold change	p-value	Klk6+/+ Mean ± SEM	Klk6−/− Mean ± SEM	Fold change	p-value
Cholesterol (ng/mg tissue)								
Total	1.1 ± 0.09	1.1 ± 0.04	0.99	-	1.1 ± 0.03	1.1 ± 0.04	1.00	-
Free	0.95 ± 0.03	1.0 ± 0.01	1.08	-	0.99 ± 0.03	1.0 ± 0.02	1.04	-
Ceramides (ng/μg protein)								
Sph	.08 ± 2.41e-3	0.10 ± 5.91e-3	1.23	-	0.08 ± 9.43e-3	0.11 ± 8.03e-3	1.42	-
SPA	0.05 ± 1.80e-3	0.06 ± 6.53e-3	1.18	-	0.02 ± 1.69e-3	0.03 ± 2.22e-3	1.50	-
S1P	0.02 ± 1.17e-3	0.01 ± 2.38e-3	0.65	-	0.01 ± 12.08e-3	0.03 ± 2.22e-3	1.54	-
C14_Cer	5.1e-3 ± 7.11e-4	8.8e-3 ± 5.83e-4	1.72	-	1.4e-5 ± 1.39e-5	2.8e-4 ± 1.3e-4	0.49	-
C16_Cer	0.02 ± 1.12e-3	0.02 ± 7.62e-4	1.28	-	9.01e-3 ± 1.0e-4	0.01 ± 1.59e-3	1.13	-
C16dh_Cer	2.8e-3 ± 9.37e-4	2.6e-3 ± 1.45e-3	0.90	-	2.26e-4 ± 2.3e-4	0.00 ± 0.00	-	-
C18_Cer	2.4 ± 0.05	2.8 ± 0.05	1.21	-	0.95 ± 0.06	1.2 ± 0.08	1.23	-
C18dh_Cer	0.32 ± 0.03	0.41 ± 0.03	1.31		0.05 ± 4.08e-3	0.05 ± 4.18e-3	0.99	
C20_Cer	0.71 ± 0.06	0.94 ± 6.39e-3	1.33	-	0.33 ± 2.84e-3	0.34 ± 7.97e-3	1.06	-
C22_Cer	3.4 ± 0.40	4.0 ± 0.27	1.16	-	1.3 ± 0.03	1.5 ± 0.04	1.14	-
C24_Cer	1.1 ± 0.11	1.3 ± 0.07	1.20	-	0.34 ± 4.19e-3	0.35 ± 3.48e-3	1.05	-
C24:1_Cer	3.9 ± 0.15	4.3 ± 0.09	1.09	-	2.6 ± 0.10	2.7 ± 0.06	1.03	-
Galactosylceramides (ng/μg protein)								
Gal_C12	0.20 ± 0.01	0.21 ± 0.01	1.05	-	0.17 ± 0.01	0.19 ± 1.00e-3	1.12	-
Gal_C16_Cer	0.35 ± 0.02	0.44 ± 0.01	1.26	-	0.28 ± 0.01	0.31 ± 0.01	1.11	-
Gal_C18_Cer	15.2 ± 0.50	17.3 ± 0.40	1.14	-	14.6 ± 0.60	15.1 ± 0.50	1.03	-
Gal_C20_Cer*	11.2 ± 0.50	13.0 ± 0.50	1.16	-	10.6 ± 0.60	11.3 ± 0.40	1.07	-
Gal_C22_Cer*	70.8 ± 2.60	78.2 ± 3.10	1.10	-	63.9 ± 3.40	67.7 ± 2.10	1.06	-
Gal_C24_Cer*	126.8 ± 4.60	134.9 ± 4.00	1.06	-	127.6 ± 6.60	134.8 ± 3.50	1.06	-
Gal_C24:1_Cer	73.7 ± 2.20	80.5 ± 1.90	1.09	-	96.2 ± 3.30	100.8 ± 1.20	1.05	-
Sphingomyelins (ng/μg protein)								
SM_C16	4.5 ± 0.34	4.3 ± 0.38	0.95	-	7.5 ± 0.29	9.8 ± 0.63	1.29	-
SM_C18:0	52.9 ± 3.72	53.1 ± 3.67	1.00	-	61.4 ± 1.70	83.8 ± 6.20	1.36	-
SM_C18:1	2.0 ± 0.12	2.1 ± 0.12	1.02	-	2.2 ± 0.06	2.8 ± 0.16	1.31	-
SM_C20:0*	2.7 ± 0.16	2.9 ± 0.11	1.06	-	2.6 ± 0.12	2.8 ± 0.05	1.09	-
SM_C22:0*	12.0 ± 0.90	12.5 ± 0.35	1.04	-	11.3 ± 0.65	12.0 ± 0.36	1.06	-
SM_C24:0	38.2 ± 2.60	35.2 ± 3.10	0.92	-	42.8 ± 2.10	56.0 ± 5.00	1.31	-

	P21				P90			
	Klk6+/+	Klk6−/−	Fold change	p-value	Klk6+/+	Klk6−/−	Fold change	p-value
	Mean ± SEM	Mean ± SEM			Mean ± SEM	Mean ± SEM		
SM_C24:1	168.4 ± 13.70	162.5 ± 14.80	0.96	-	231.7 ± 12.40	298.7 ± 22.80	1.29	-

Table shows quantification of lipid species and fold change from Klk6−/− relative to wild type (i.e. value >1 are species increased in KLK6−/−) in the myelin-enriched fragment isolated from female P21 or P90 spinal cord. The myelin fraction from Klk6−/− mice shows no change in abundance of cholesterol relative to wild-type at either timepoint. In general, ceramides trended to be increased in Klk6−/− compared to wild type, particularly at P21, with differences between genotypes tending to diminish by P90. In contrast, sphingomyelin content is very similar between genotypes at the peak of myelination (P21), and tends to become more abundant in Klk6−/− spinal cord myelin by P90. These differences highlight differential regulation of myelin lipid species throughout the lifespan. Galactosylceramides show stable abundance in the myelin enriched fragment both through time and across genotypes. N = 3 per genotype, per timepoint. All P values were adjusted for multiple comparisons with the Benjamini-Hochberg method with a false discovery rate of 0.05, non-significant P values not reported.

* indicates lipid species which did not have a standard available; data was normalized by area ration of analyte/internal standard.